

BAW-1699

December 1981

ANALYSIS OF CAPSULE OCII-A FROM
DUKE POWER COMPANY'S
OCONEE NUCLEAR STATION, UNIT 2

— Reactor Vessel Material Surveillance Program —

8201250101 820112
PDR ADDCK 05000269
P PDR

Babcock & Wilcox
a McDermott company

ANALYSIS OF CAPSULE OCII-A FROM
DUKE POWER COMPANY'S
OCONEE NUCLEAR STATION, UNIT 2

- Reactor Vessel Material Surveillance Program -

by

A. L. Lowe, Jr., PE
J. W. Ewing
W. A. Pavinich
W. L. Redd
J. K. Schmotzer

B&W Contract No. 582-7109-71

BABCOCK & WILCOX
Nuclear Power Group
Nuclear Power Generation Division
P. O. Box 1260
Lynchburg, Virginia 24505

SUMMARY

This report describes the results of the examination of the second capsule of Duke Power Company's Oconee Unit 2 reactor vessel surveillance program. The capsule was removed and examined after accumulating a fluence of 3.37×10^{18} nvt, which is equivalent to approximately 16 effective full-power years (EFPY). The objective of the program is to monitor the effects of neutron irradiation on the tensile and fracture toughness properties of the reactor pressure vessel materials by testing and evaluating tensile, Charpy impact, and compact fracture toughness specimens. The program was designed in accordance with the requirements of Appendix H to 10 CFR 50¹ and ASTM specification E185-73.

The capsule received an average fast fluence of 3.37×10^{18} n/cm² (E > 1 Mev), and the predicted fast fluence for the reactor vessel T/4 location at the end of 3.7 EFPY operation is 9.8×10^{17} n/cm² (E > 1 Mev). Based on the calculated current fast flux at the vessel inside wall and an 80% load factor, the projected fast fluence the Oconee Unit 2 reactor pressure vessel will receive in 40 calendar years of operation is 1.20×10^{19} n/cm² (E > 1 Mev).

The results of the tensile tests indicated that the materials exhibited normal behavior relative to neutron fluence exposure. The Charpy impact results exhibited the characteristic behavior of a shift to higher temperature for both the 30- and 50-ft-lb transition temperatures as a result of neutron fluence damage and a decrease in upper shelf energy. These results demonstrated that the current techniques used for predicting the change in both the increase in the RT_{NDT} and the decrease in upper shelf properties due to irradiation are conservative.

The recommended operating period was extended to 15 EFPY as a result of the second capsule evaluation. These new operating limitations are in accordance with the requirements of 10 CFR 50, Appendix G.

1. INTRODUCTION

This report describes the results of the examination of the second capsule of Duke Power Company's Oconee Nuclear Station, Unit 2 reactor vessel surveillance program. The first capsule from this program was removed and examined after the first year of operation; the results are reported in BAW-1437.²

The objective of the program is to monitor the effects of neutron irradiation on the tensile and impact properties of reactor pressure vessel materials under actual operating conditions. The surveillance program for Oconee 2 was designed and furnished by Babcock & Wilcox; it is described in BAW-10006A.³ The program was planned to monitor the effects of neutron irradiation on the reactor vessel materials for the 40-year design life of the reactor pressure vessel.

The surveillance program for Oconee 2 was designed in accordance with E185-66 and thus does not comply with Appendixes G and H to 10 CFR 50 since the requirements did not exist at the time the program was designed. Because of this difference, additional tests and evaluations were required to ensure meeting the requirements of 10 CFR 50, Appendixes G and H. The recommendations for the future operation of Oconee 2 included in this report do comply with these requirements.

2. BACKGROUND

The ability of the reactor pressure vessel to resist fracture is the primary factor in ensuring the safety of the primary system in light water cooled reactors. The beltline region of the reactor vessel is the most critical region of the vessel because it is exposed to neutron irradiation. The general effects of fast neutron irradiation on the mechanical properties of such low-alloy ferritic steels as SA508, Class 2 forgings used in the fabrication of the Oconee 2 reactor vessel are well characterized and documented in the literature. The low-alloy ferritic steels used in the beltline region of reactor vessels exhibit an increase in ultimate and yield strength properties after irradiation, with a corresponding decrease in ductility. The most serious mechanical property change in reactor pressure vessel steels is the increase in temperature for the transition from brittle to ductile fracture accompanied by a reduction in the upper shelf impact strength.

Appendix G to 10 CFR 50, "Fracture Toughness Requirements," specifies minimum fracture toughness requirements for the ferritic materials of the pressure-retaining components of the reactor coolant pressure boundary (RCPB) of water-cooled power reactors and provides specific guidelines for determining the pressure-temperature limitations on operation of the RCPB. The toughness and operational requirements are specified to provide adequate safety margins during any condition of normal operation, including anticipated operational occurrences and system hydrostatic tests, to which the pressure boundary may be subjected over its service lifetime. Although the requirements of Appendix G to 10 CFR 50 became effective on August 13, 1973, the requirements are applicable to all boiling and pressurized water-cooled nuclear power reactors, including those under construction or in operation on the effective date.

Appendix H to 10 CFR 50, "Reactor Vessel Material Surveillance Program Requirements," defines the material surveillance program required to monitor changes in the fracture toughness properties of ferritic materials in the reactor vessel beltline region of water-cooled reactors resulting from exposure to neutron

irradiation and the thermal environment. Fracture toughness test data are obtained from material specimens withdrawn periodically from the reactor vessel. These data will permit determination of the conditions under which the vessel can be operated with adequate safety margins against fracture throughout its service life.

A method for guarding against brittle fracture in reactor pressure vessels is described in Appendix G to the ASME Boiler and Pressure Vessel Code, Section III. This method utilizes fracture mechanics concepts and the reference nil-ductility temperature, RT_{NDT} , which is defined as the greater of the drop weight nil-ductility transition temperature (per ASTM E-208) or the temperature that is 60F below that at which the material exhibits 50 ft-lb and 35 mils lateral expansion. The RT_{NDT} of a given material is used to index that material to a reference stress intensity factor curve (K_{IR} curve), which appears in Appendix G of ASME Section III. The K_{IR} curve is a lower bound of dynamic, static, and crack arrest fracture toughness results obtained from several heats of pressure vessel steel. When a given material is indexed to the K_{IR} curve, allowable stress intensity factors can be obtained for this material as a function of temperature. Allowable operating limits can then be determined using these allowable stress intensity factors.

The RT_{NDT} and, in turn, the operating limits of a nuclear power plant, can be adjusted to account for the effects of radiation on the properties of the reactor vessel materials. The radiation embrittlement and the resultant changes in mechanical properties of a given pressure vessel steel can be monitored by a surveillance program in which a surveillance capsule containing prepared specimens of the reactor vessel materials is periodically removed from the operating nuclear reactor and the specimens tested. The increase in the Charpy V-notch 50-ft-lb temperature, or the increase in the 35 mils of lateral expansion temperature, whichever results in the larger temperature shift due to irradiation, is added to the original RT_{NDT} to adjust it for radiation embrittlement. The adjusted RT_{NDT} is used to index the material to the K_{IR} curve which, in turn, is used to set operating limits for the nuclear power plant. These new limits take into account the effects of irradiation on the reactor vessel materials.

3. SURVEILLANCE PROGRAM DESCRIPTION

The surveillance program for Oconee 2 comprises six surveillance capsules designed to monitor the effects of the neutron and thermal environment on the materials of the reactor pressure vessel core region. The capsules, which were inserted into the reactor vessel before initial plant startup, were positioned inside the vessel between the thermal shield and the vessel wall at the locations shown in Figure 3-1. Two capsules were placed in each holder tube and positioned near the peak axial and azimuthal neutron flux. BAW-10006A includes a full description of capsule locations and design.³ After the capsules were removed from Oconee Unit 2 and were included in the integrated reactor vessel material surveillance program, they were irradiated in the Crystal River Unit 3 reactor. During this period of irradiation Capsule OCII-A was irradiated in site yz as shown in Figure 3-2.

Capsule OCII-A was removed from Crystal River Unit 3 after cycle 2 and an accumulated fluence of approximately 3×10^{18} nvt. This capsule contained Charpy V-notch impact and tensile specimens fabricated of SA508, Class 2 steel, weld metal, and correlation steel. The specimens contained in the capsule are described in Table 3-1, and the chemistry and heat treatment of the surveillance material are described in Table 3-2.

The capsule contained longitudinal Charpy V-notch specimens from correlation material obtained from plate 02 of the USAEC Heavy Section Steel Technology Program. This 12-inch-thick plate of ASTM 533, Grade B, Class 1 steel was produced by the Luken Steel Company (heat A-1195-1) and heat-treated by Combustion Engineering. The chemistry and heat treatment of the correlation material are described in Table 3-3.

All test specimens were machined from the 1/4-thickness location of the shell forging. Charpy V-notch and tensile specimens from the vessel material were oriented with their longitudinal axes parallel to the principal working direction of the forgings; the specimens were also oriented transverse to the

Table 3-2. Chemistry and Heat Treatment
of Surveillance Materials

Chemical Analysis

<u>Element</u>	<u>Heat AAW-163</u>	<u>Weld metal WF-209-1A</u>
C	0.24	0.057
Mn	0.63	1.58
P	0.006	0.020
S	0.012	0.005
Si	0.25	0.56
Ni	0.75	0.48
Mo	0.62	0.33
Cu	0.04	0.30

Heat Treatment

<u>Heat No.</u>	<u>Temp, F</u>	<u>Time, h</u>	<u>Cooling</u>
AAW-163	1620-1660	4.0	Cold water quench
	1570-1610	4.0	Cold water quench
	1240-1280	10.0	Cold water quench
	1100-1150	40.0	Furnace-cooled
WF-209-1A	1100-1150	33.0	Furnace-cooled

Table 3-3. Chemistry and Heat Treatment of Correlation Material - Heat A-1195-1, A533 Grade B, Class 1 (HSST Plate 02)

Chemical Analysis (1/4T) ^(a)

<u>Element</u>	<u>Wt %</u>
C	0.23
Mn	1.39
P	0.013
S	0.013
Si	0.21
Ni	0.64
Mo	0.50
Cu	0.17

Heat Treatment ^(b)

1. Normalized at 1675F ± 75F.
2. 1600F ± 75F for 4 h/water-quenched.
3. 1225F ± 25F for 4 h/furnace-cooled.
4. 1125F ± 25F for 40 h/furnace-cooled.

(a) ORNL-4463.

(b) Per plate section identification card.

Figure 3-1. Reactor Vessel Cross Section Showing Surveillance Capsule Locations at Oconee Unit 2

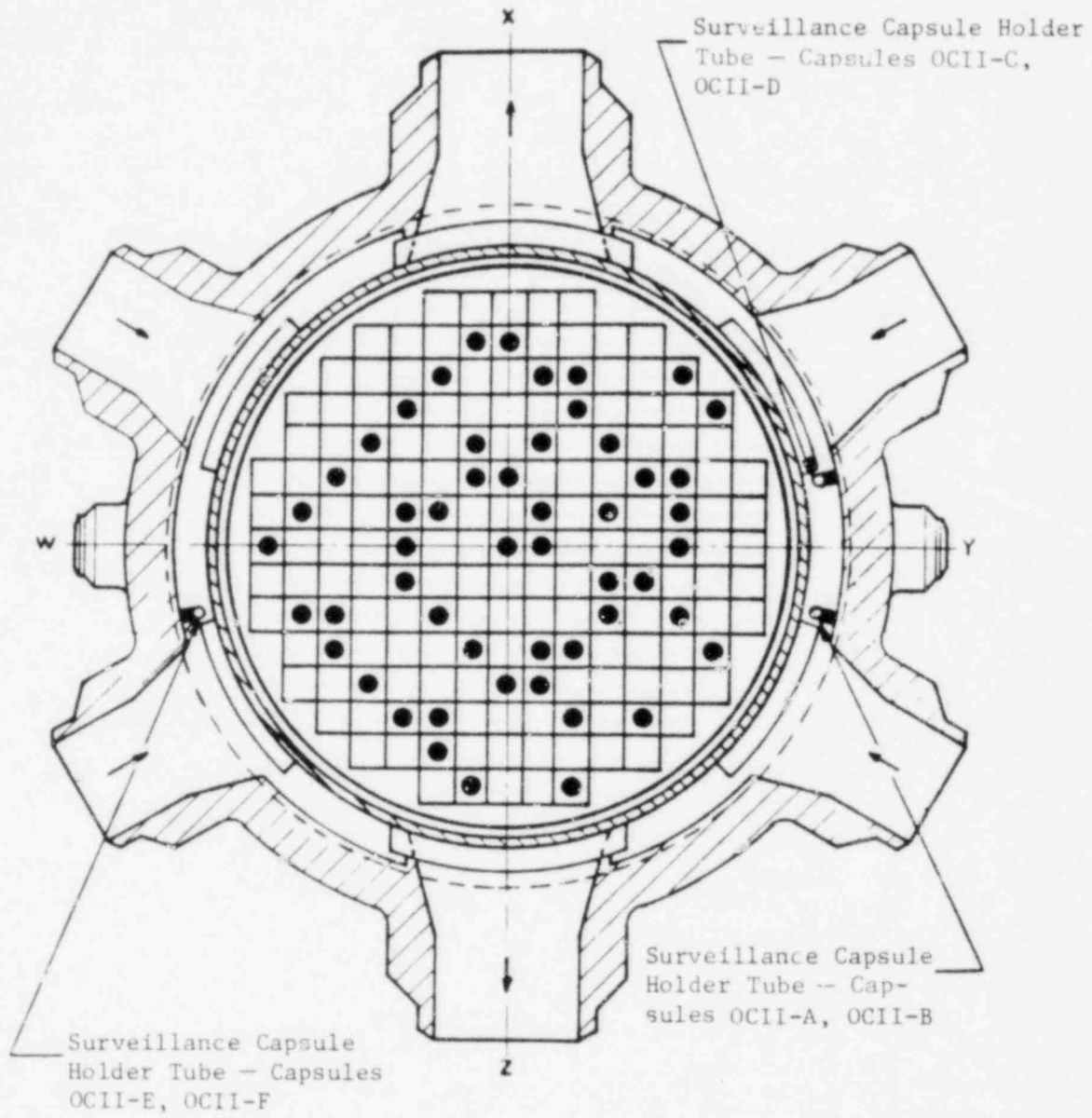
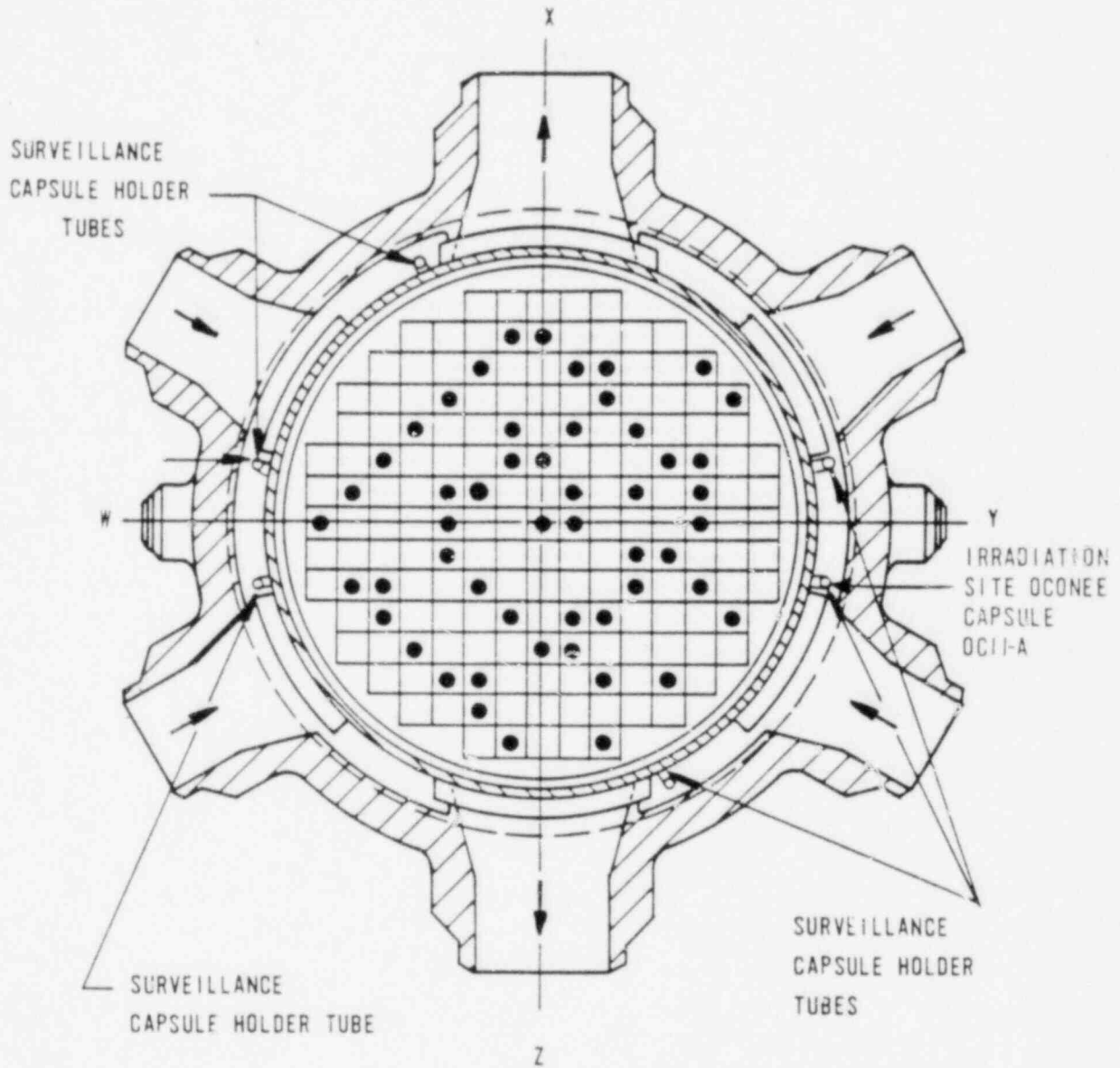


Figure 3-2. Reactor Vessel Cross Section Showing Location of Oconee Unit 2 Capsule OCII-A in Crystal River Unit 3 Reactor



4. PREIRRADIATION TESTS

Unirradiated material was evaluated for two purposes: (1) to establish a baseline of data to which irradiated properties data could be referenced, and (2) to determine to the extent practical from available material, the material properties as required for compliance with Appendixes G and H to 10 CFR 50.

4.1. Tensile Tests

Tensile specimens were fabricated from the reactor vessel shell course plate and weld metal. The subsize specimens were 4.25 inches long with a reduced section 1.750 inches long by 0.357 inch in diameter. They were tested on a 55,000-lb load capacity universal test machine at a crosshead speed of 0.050 inch per minute. A four-pole extension device with a strain-gaged extensometer was used to determine the 0.2% yield point. Test conditions were in accordance with the applicable requirements of ASTM A370-72. For each material type and/or condition, six specimens in groups of three were tested at both room temperature and 580F. The tension-compression load cell used had a certified accuracy of better than $\pm 0.5\%$ of full scale (25,000 lb). All test data for the pre-irradiation tensile specimens are given in Appendix B.

4.2. Impact Tests

Charpy V-notch impact tests were conducted in accordance with the requirements of ASTM Standard Methods A370-72 and E23-72 on an impact tester certified to meet Watertown standards. Test specimens were of the Charpy V-notch type, which were nominally 0.394 inch square and 2.165 inches long.

Prior to testing, specimens were temperature-controlled in liquid immersion baths capable of covering the temperature range from -85 to +600F. Specimens were removed from the baths and positioned in the test frame anvil with specially designed tongs. The pendulum (hammer) was released manually, allowing the specimens to be broken within 5 seconds after their removal from the temperature baths.

Impact test data for the unirradiated baseline reference materials are presented in Appendix C. Tables C-1 through C-4 contain the basic data, which are plotted in Figures C-1 through C-4.

5. POSTIRRADIATION TESTS

5.1. Thermal Monitors

Surveillance capsule OCII-A contained three temperature monitor holder tubes, each containing five fusible alloys with different melting points ranging from 558 to 621F. All the thermal monitors at 558, 580, 588, and 610F had melted, while those at 621F remained in their original configuration as initially placed in the capsule except for slight signs of slumping. From these data it was concluded that the irradiated specimens had been exposed to a maximum temperature in the range from 610 to less than 621F during the reactor vessel period. This higher (than anticipated) temperature occurred because these capsules were designed for lower lead factor capsule positions. The higher lead factor in the Crystal River Unit 3 radiation site would cause a slight increase in gamma heating, which in turn could cause the increase in temperature detected by the thermal monitors. There appeared to be no significant temperature gradient along the capsule length.

5.2. Tensile Test Results

The results of the postirradiation tensile tests are presented in Table 5-1. Tests were performed on specimens at both room temperature and 580F using the same test procedures and techniques used to test the unirradiated specimens (section 4.1). In general, the ultimate strength and yield strength of the material increased slightly with a corresponding slight decrease in ductility; both effects were the result of neutron radiation damage. The type of behavior observed and the degree to which the material properties changed are within the range of changes to be expected for the radiation environment to which the specimens were exposed.

The results of the preirradiation tensile tests are presented in Appendix B.

5.3. Charpy V-Notch Impact Test Results

The test results from the irradiated Charpy V-notch specimens of the reactor vessel beltline material and the correlation monitor material are presented in

Tables 5-2 through 5-6 and Figures 5-1 through 5-5. The test procedures and techniques were the same as those used to test the unirradiated specimens (section 4.2). The material exhibited a sensitivity to irradiation within the values predicted from its chemical composition and the fluence to which it was exposed.

The results of the preirradiation Charpy V-notch impact test are given in Appendix C.

Table 5-1. Irradiation Tensile Properties of Capsule OCII-A Base Metal and Weld Metal Irradiated to 3.37×10^{18} nvt (E > 1.0 Mev)

Specimen No.	Test temp, F	Strength, psi		Elongation, %		Red'n in area, %
		Yield	Ult.	Unif	Total	
<u>Base Metal, Longitudinal -- Heat AAW-163</u>						
EE-715	69	72,500	94,400	14.0	27.1	68.9
EE-717	69	70,300	91,900	14.1	30.6	68.9
Mean	69	71,400	93,150	14.05	28.85	68.9
Std dev'n		1,550	1,770	0.07	2.47	0
EE-703	579	63,800	86,300	12.5	24.3	67.3
EE-712	582	65,600	87,500	13.7	25.5	68.9
Mean	580	64,700	86,900	13.57	24.9	68.1
Std dev'n		1,270	850	0.74	0.85	1.13
<u>Weld Metal -- WF-209-1</u>						
EE-115	69	96,300	110,000	14.9	24.9	57.0
EE-117	69	99,400	111,300	15.3	17.1	29.8
Mean	69	97,850	110,650	15.1	21.0	43.4
Std dev'n		2,190	920	0.28	5.52	19.23
EE-103	584	86,300	103,100	12.1	22.6	43.5
EE-121	581	86,200	101,300	12.2	18.3	44.4
Mean	580	86,250	102,200	12.15	20.45	43.95
Std dev'n		70	1,270	0.07	3.04	0.64

Table 5-2. Irradiated Charpy Impact Data for Capsule OCII-A
Irradiated to 3.37×10^{18} nvt, Base Metal HAZ,
Longitudinal Orientation

Specimen No.	Test temp, F	Absorbed energy, ft-lb	Lateral expansion, 10^{-3} in.	Shear fracture, %
EE-413	-80	62.5	47.0	30
EE-401	-35	78.5	47.0	20
EE-414	0	93.5	63.5	30
EE-415	38	51.0	40.0	70
EE-439	75	117.0	77.0	50
EE-419	140	127.5	94.0	100
EE-436	224	139.0	93.0	100
EE-424	440	115.0	83.5	100

Table 5-3. Irradiated Charpy Impact Data for Capsule OCII-A
Irradiated to 3.37×10^{18} nvt, Base Metal,
Transverse Orientation

Specimen No.	Test temp, F	Absorbed energy, ft-lb	Lateral expansion, 10^{-3} in.	Shear fracture, %
EE-609	-1	41.5	34.0	5
EE-602	38	73.5	51.0	15
EE-614	40	53.5	41.5	5
EE-621	75	97.5	66.5	30

Table 5-4. Irradiated Charpy Impact Data for Capsule OCII-A
Irradiated to 3.37×10^{18} nvt, Base Metal,
Longitudinal Orientation

Specimen No.	Test temp, F	Absorbed energy, ft-lb	Lateral expansion, 10^{-3} in.	Shear fracture, %
EE-715	-40	22.0	15.5	0
EE-723	-20	56.5	41.0	10
EE-737	0	41.5	29.0	0
EE-704	19	69.0	53.5	30
EE-714	75	108.0	72.5	75
EE-707	140	122.0	81.5	85
EE-731	224	134.0	87.5	100
EE-739	400	126.0	94.0	100

Table 5-5. Irradiated Charpy Impact Data for Capsule OCII-A
Irradiated to 3.37×10^{18} nvt, Weld Metal

Specimen No.	Test temp, F	Absorbed energy, ft-lb	Lateral expansion, 10^{-3} in.	Shear fracture, %
EE-013	38	17.5	18.5	10
EE-003	75	19.0	28.5	20
EE-021	110	32.0	33.0	65
EE-039	140	33.0	34.5	90
EE-029	193	42.0	48.0	100
EE-002	226	46.5	44.0	100
EE-005	284	46.0	46.0	100
EE-033	408	44.5	44.0	100

Table 5-6. Irradiated Charpy Impact Data for Capsule OCII-A
 Irradiated to 3.37×10^{18} nvt, Correlation Material

Specimen No.	Test temp, F	Absorbed energy, ft-lb	Lateral expansion, 10^{-3} in.	Shear fracture, %
EE-950	72	12.5	9.5	2
EE-942	110	25.5	21.0	30
EE-903	120	33.0	29.5	15
EE-904	130	27.0	32.0	30
FE-934	140	62.0	52.5	35
EE-919	204	84.5	64.0	100
EE-914	318	103.0	84.0	100
EE-935	440	102.5	77.5	100

Figure 5-1. Impact Data From Irradiated Base Metal (AAW-163) HAZ, Longitudinal Orientation

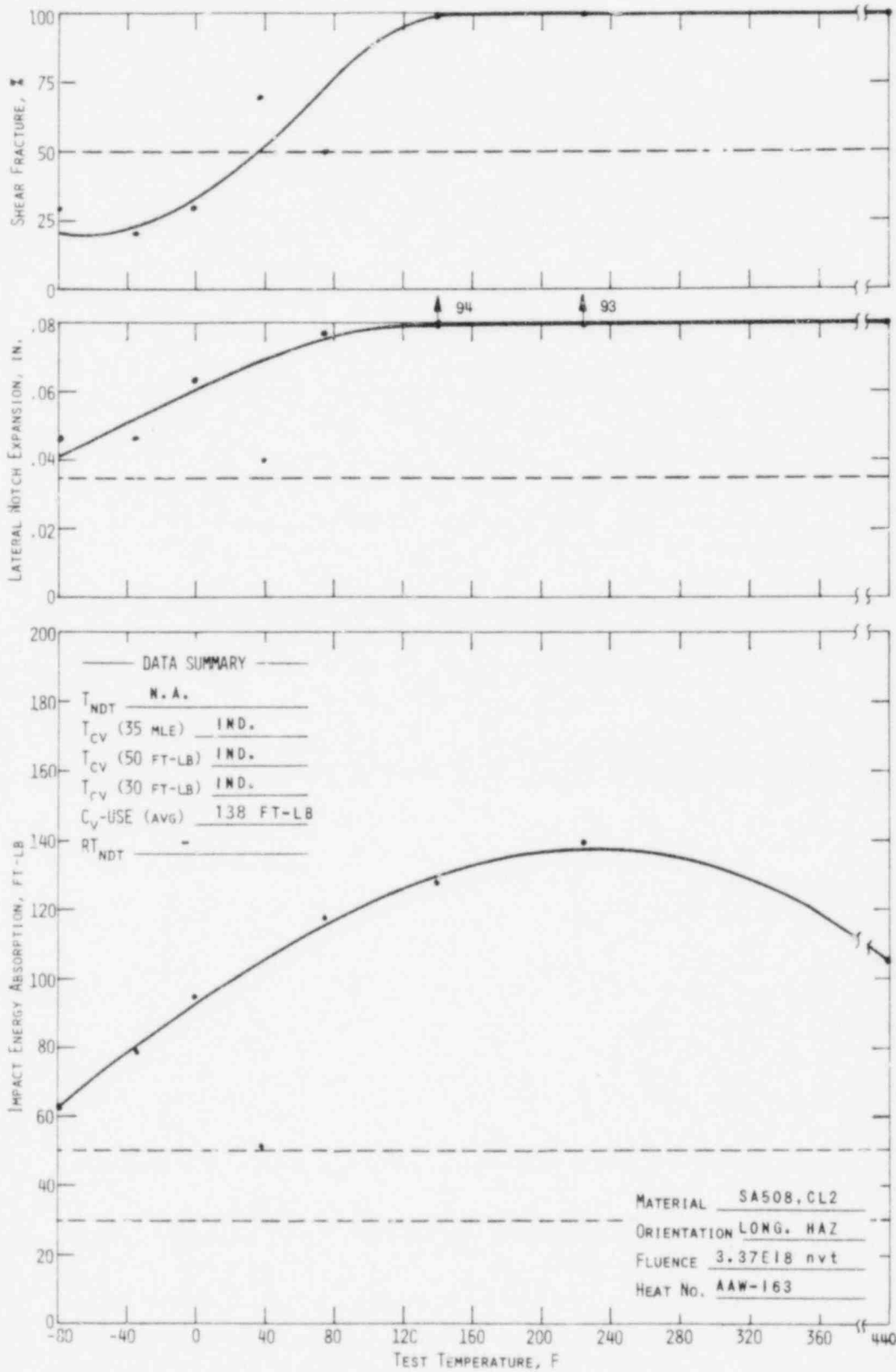


Figure 5-2. Impact Data From Irradiated Base Metal (AAW-163), Transverse Orientation

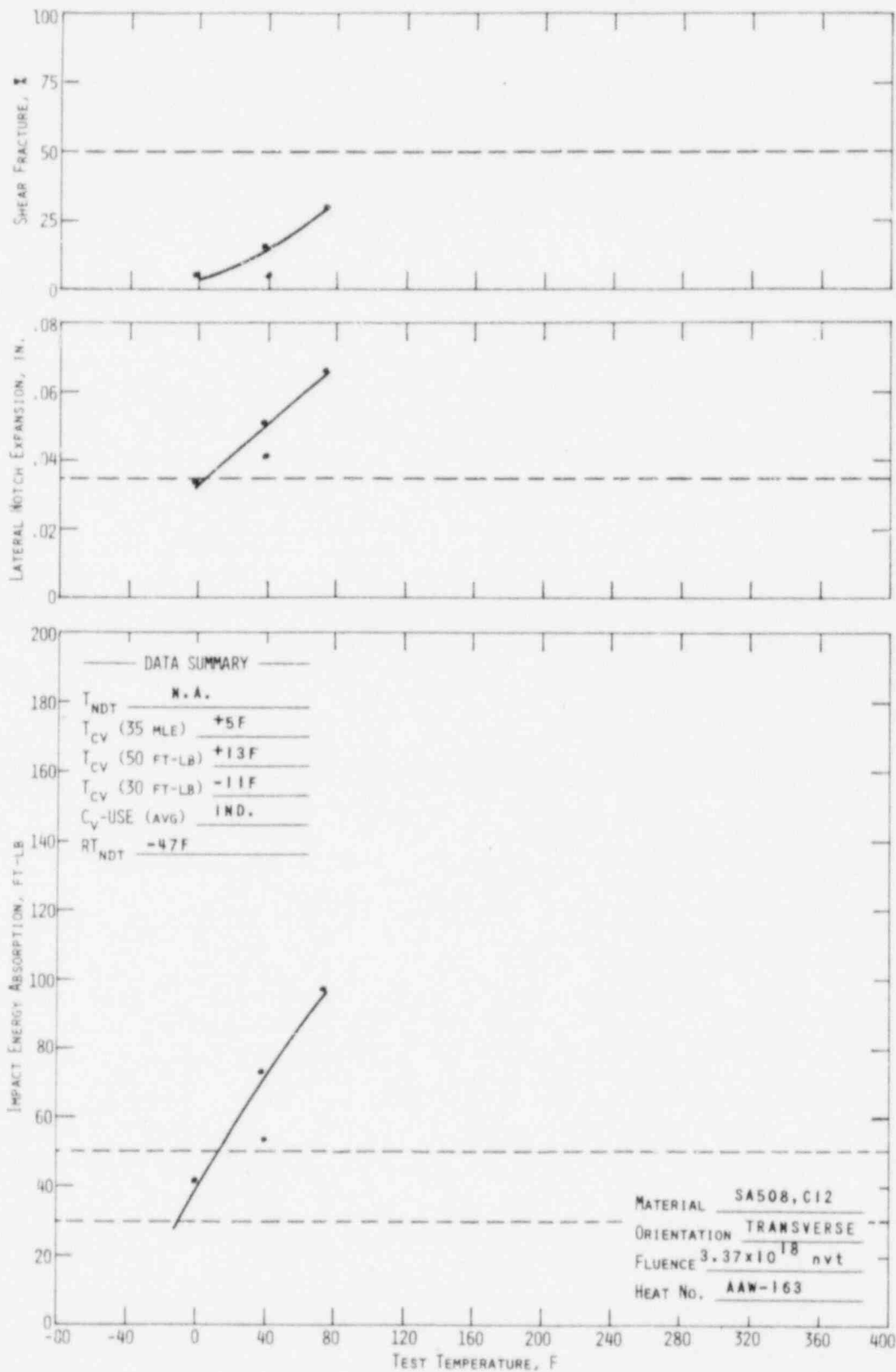


Figure 5-3. Impact Data From Irradiated Base Metal (AAW-163), Longitudinal Orientation

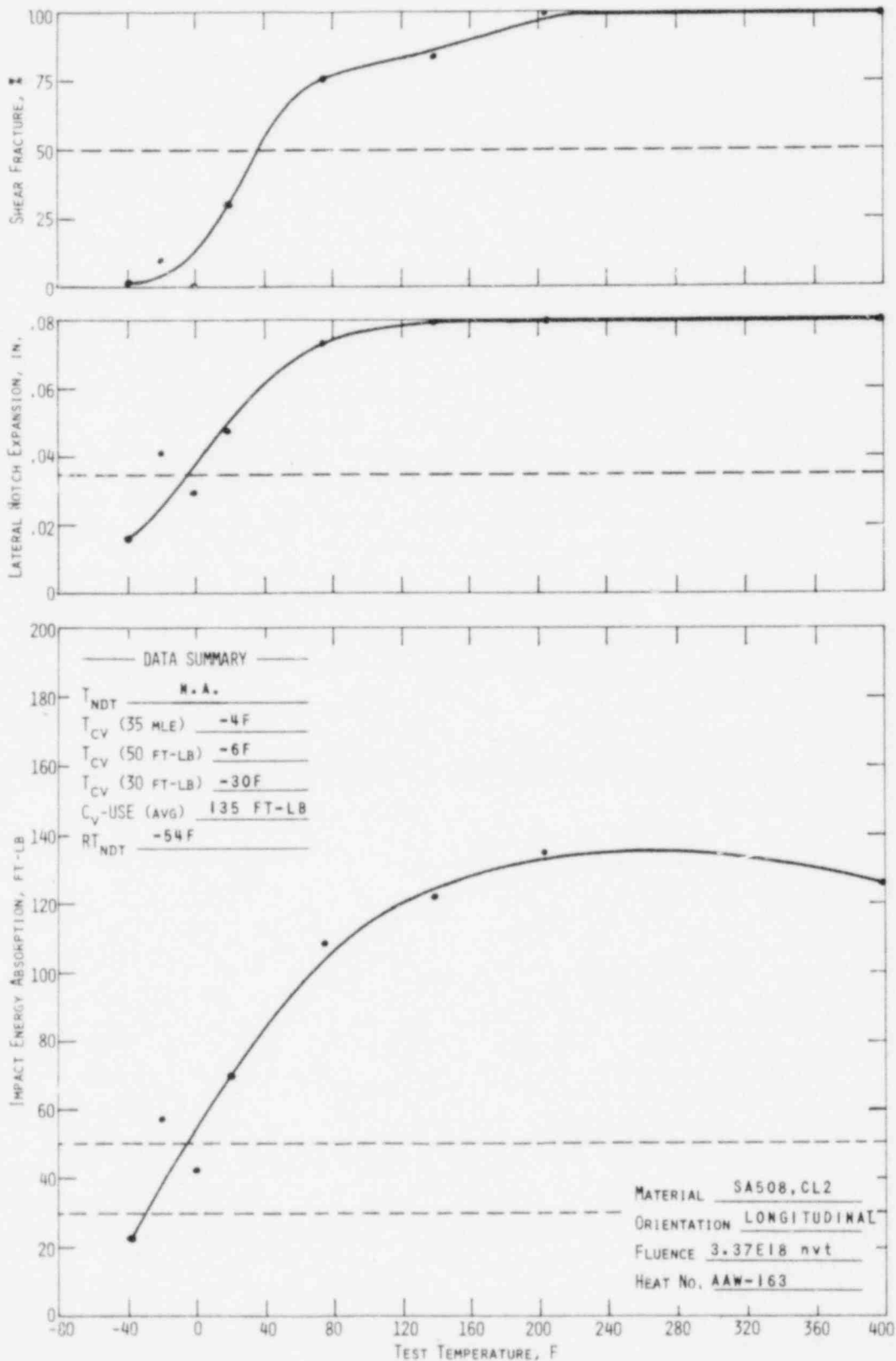


Figure 5-4. Impact Data From Irradiated Weld Metal (WF-209-1)

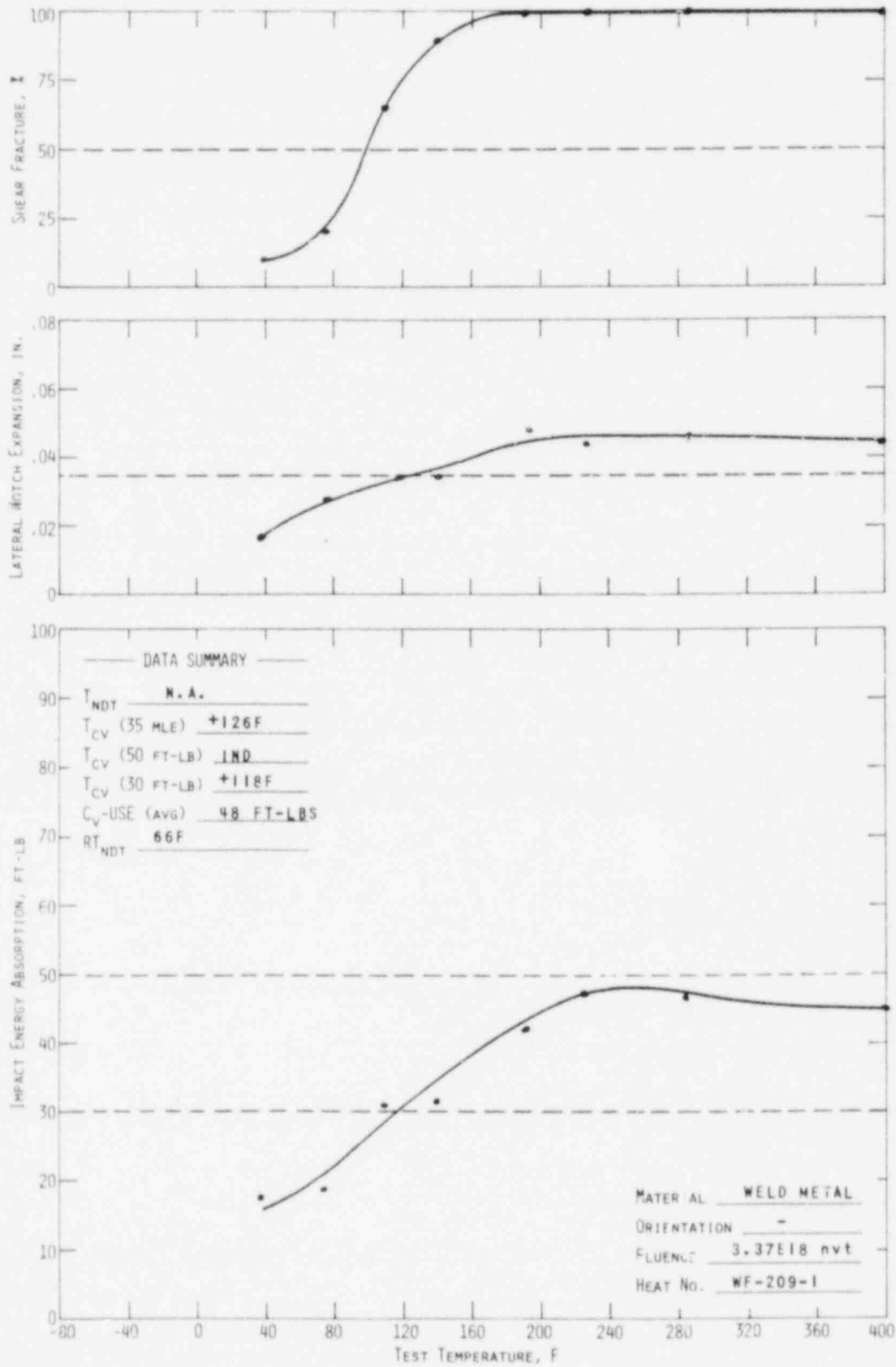
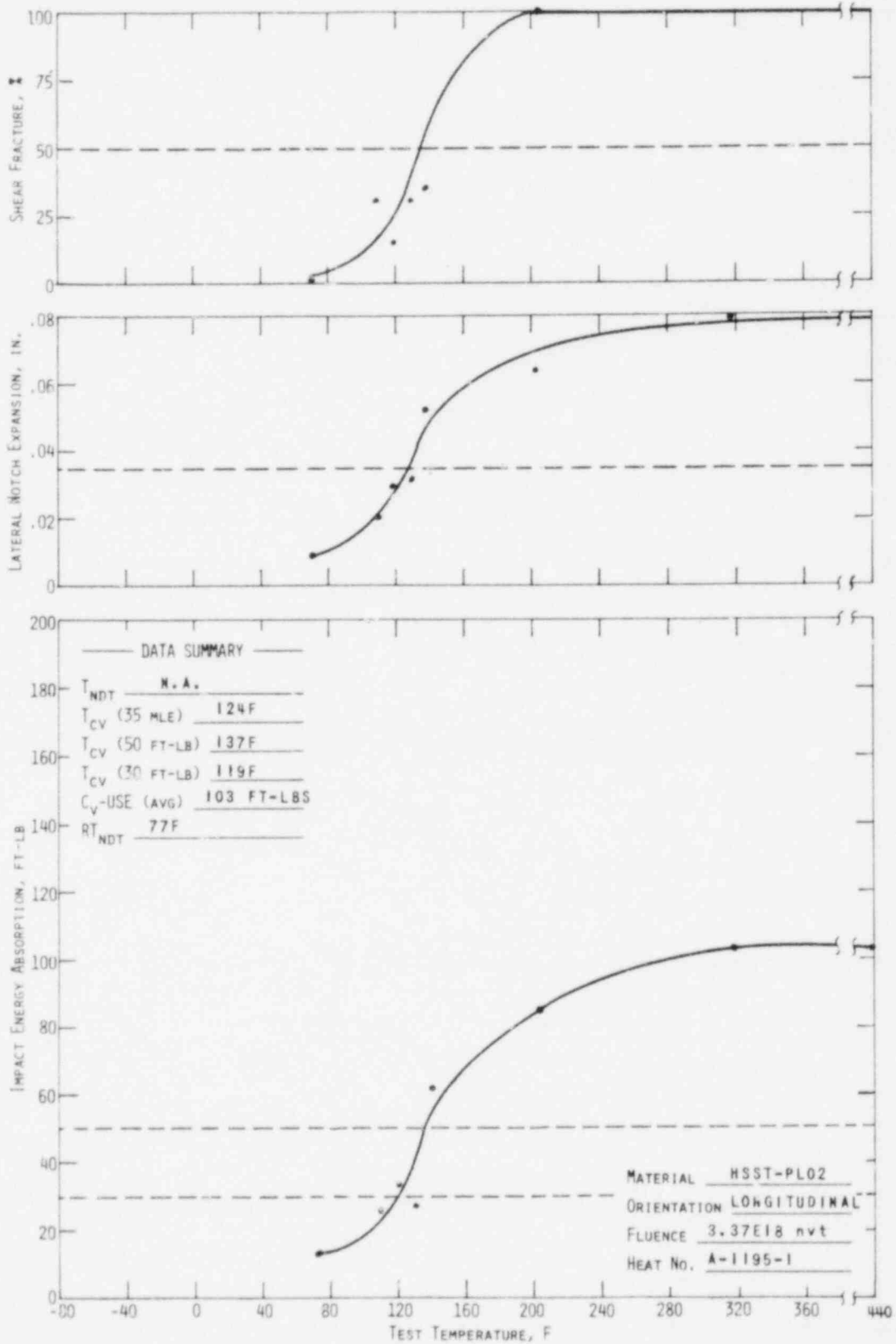


Figure 5-5. Impact Data From Irradiated Correlation Material (HSST Plate 02)



6. NEUTRON DOSIMETRY

6.1. Background

As a part of the pressure vessel surveillance program, fluence analysis has three primary objectives: (1) determination of maximum fluence at the pressure vessel as a function of reactor operation, (2) prediction of pressure vessel fluence in the future, and (3) determination of the test specimen fluence within the surveillance capsule. Vessel fluence data are used to evaluate changes in reference transition temperature and upper shelf energy levels and to establish pressure-temperature operation curves. Test specimen fluence data are used to establish the correlation between changes in material properties and fluence exposure. To provide this information, a model for calculating flux distributions in the reactor is established. The accuracy of calculated fast flux is enhanced by the use of a normalization factor which utilizes measured activity data obtained from capsule dosimeters. A significant aspect of the surveillance program is to provide a correlation between the neutron fluence above 1 Mev and the radiation-induced property changes noted in the surveillance specimens. To permit such a correlation, activation detectors with reaction thresholds in the energy range of interest were placed in each surveillance capsule. The significant properties of the detectors are given in Table 6-1.

Because of a long half-life (30 years) and an effective threshold energy of 0.5 Mev, the measurements of ^{137}Cs production from fission reactions in ^{237}Np (and ^{238}U) are more directly applicable to analytical determinations of the fast neutron fluence ($E > 1$ Mev) for multiple fuel cycles than the other dosimeter reactions. The other dosimeter reactions are useful as corroborating data for shorter time intervals and/or higher energy fluxes. Short-lived isotope activities are representative of reactor conditions only over the latter portion of the irradiation period (fuel cycle), whereas reactions with a threshold energy higher than 2 or 3 Mev do not record a significant part of the total fast flux.

The energy-dependent neutron flux is not directly available from activation detectors because the dosimeters register only the integrated effect of the neutron flux on the target material as a function of both irradiation time and neutron energy. To obtain an accurate estimate of the average neutron flux incident upon the detector, several parameters must be known: the operating history of the reactor, the energy response of the given detector, and the neutron spectrum at the detector location. Of these parameters, the definition of the neutron spectrum is the most difficult to obtain. Essentially two means are available to obtain it: iterative unfolding of experimental dosimeter data and/or analytical methods. Because of a lack of sufficient threshold reaction detectors that satisfy both the threshold energy and half-life requirements of a surveillance program, calculated spectra are used in this analysis.

Neutron transport calculations in two-dimensional geometry are used to calculate energy-dependent flux distributions throughout the reactor. Reactor conditions are selected to be representative of an average over the irradiation time period. Geometric details are selected to explicitly represent the surveillance capsule assembly and the pressure vessel. The detailed calculational procedure is described in Appendix D.

6.2. Vessel Fluence

The maximum fluence ($E > 1.0$ Mev) in the Oconee 2 pressure vessel through cycle 4 was determined to be $1.77 (+18)$ n/cm² based on an average neutron flux of $1.57 (+10)$ n/cm²-s for cycles 2, 3, and 4 and $1.39 (+10)$ n/cm²-s for cycle 1 (Tables 6-2 and 6-3). The location of maximum fluence is a point at the cladding/vessel interface at an elevation about 100 cm above the lower active fuel boundary and an azimuthal (peripheral) location of about 12° from a major axis (across flats diameter). Fluence data have been extrapolated to 32 EFPY of operation based on the premise that ex-core flux is proportional to fast flux that escapes the reactor core (Appendix D). Core escape flux values are available from fuel management analyses of future fuel cycles.

Relative fluence as a function of radial location in the pressure vessel is shown in Figure 6-1. Corresponding lead factors from the cladding interface to T/4, T/2, and 3T/4 are 1.8, 3.7, and 7.9, respectively. Relative fluence as a function of azimuthal angle is shown in Figure 6-2. A peak occurs at about 12°, which roughly corresponds to a corner of the core and to three

symmetric capsule locations. Two other capsule locations correspond to the azimuthal minimum at about 26° . However, it should be noted that the maximum: minimum flux ratio is only 1.3, and the data in Figure 6-2 do not account for flux perturbation by the capsule itself. Fast neutron flux is increased by approximately 1.25 in the capsule due to differences in scattering and absorption cross sections between steel and water, i.e., model with and without capsule.

6.3. Capsule Fluence

Fluence at the center of the surveillance capsule was calculated to be $3.37 (+18) \text{ n/cm}^2$, about 28% of which was received in Oconee 2 and about 72% in Crystal River 3 (Table 6-4). These data represent average values in the capsule. Capsule OCII-A was located in an upper holder tube position 11° off axis and approximately 211 cm from the core center for 440 EFPD in Oconee Unit 2, cycle 1. (This corresponds to the original 177-fuel assembly holder tube design.) It was then inserted in Crystal River 3 in an upper holder tube position 11° off axis and about 202 cm from the core axis for an additional 338 EFPD. During the latter irradiation period, the capsule was estimated to have been rotated 110° clockwise relative to its original design orientation (key facing the reactor core).

Table 6-1. Surveillance Capsule Detectors

Detector reaction	Effective lower energy limit, Mev	Isotope half-life
$^{54}\text{Fe}(n,p)^{54}\text{Mn}$	2.5	312.5 d
$^{58}\text{Ni}(n,p)^{58}\text{Co}$	2.3	70.85 d
$^{238}\text{U}(n,f)^{137}\text{Cs}$	1.1	30.03 yr
$^{237}\text{Np}(n,f)^{137}\text{Cs}$	0.5	30.03 yr
$^{238}\text{U}(n,f)^{106}\text{Ru}$	1.1	368.2 d
$^{237}\text{Np}(n,f)^{106}\text{Ru}$	0.5	369 d
$^{238}\text{U}(n,f)^{103}\text{Ru}$	1.1	39.43 d
$^{237}\text{Np}(n,f)^{103}\text{Ru}$	0.5	39.43 d
$^{238}\text{U}(n,f)^{144}\text{Ce}$	1.1	284.4 d
$^{237}\text{Np}(n,f)^{144}\text{Ce}$	0.5	284.4 d
$^{238}\text{U}(n,f)^{95}\text{Zr}$	1.1	64.1 d
$^{237}\text{Np}(n,f)^{95}\text{Zr}$	0.5	64.1 d

Table 6-2. Pressure Vessel Flux

Cycle	Fast flux, n/cm ² -s (E > 1 Mev)		Flux, n/cm ² -s (E > 0.1 Mev) Inside surface (max location)	
	Inside surface (max location)	T/4		3T/4
Cycle 1 ^(a) , 440 EFPD	1.39(+10)	7.9(+9)	1.8(+9)	2.74(+10)
Cycles 2,3,4, 921.2 EFPD	1.57(+10)	8.6(+9)	2.0(+9)	3.34(+10)

(a) Data from reference 1.

Table 6-3. Pressure Vessel Fluence

Cumulative irradiation time	Fast fluence, n/cm^2 ($E > 1$ Mev)		
	Inside surface (max location)	T/4	3T/4
End of cycle 1 ^(a) (440 EFPD)	5.28(+17)	2.9(+17)	6.6(+16)
End of cycle 4 (1361 EFPD)	1.77(+18)	9.8(+17)	2.3(+17)
15 EFPY	5.83(+18)	3.2(+18)	7.3(+17)
32 EFPY	1.20(+19)	6.7(+18)	1.5(+18)

(a) Data from reference 1.

Table 6-4. Surveillance Capsule Fluence

	Flux, n/cm^2-s ($E > 1$ Mev)	Fluence n/cm^2	Cumulative fluence, n/cm^2	Flux, n/cm^2-s ($E > 0.1$ Mev)
OC 2, cycle 1 ^(a) , 440 EFPD	2.48(+10)	9.43(+17)	9.43(+17)	4.66(+10)
CR-3, cycles 1B and 2, 338 EFPD	8.34(+10)	2.43(+18)	3.37(+18)	1.96(+11)

(a) Data from reference 1.

Figure 6-1. Radial Fluence Gradient Through Reactor Vessel

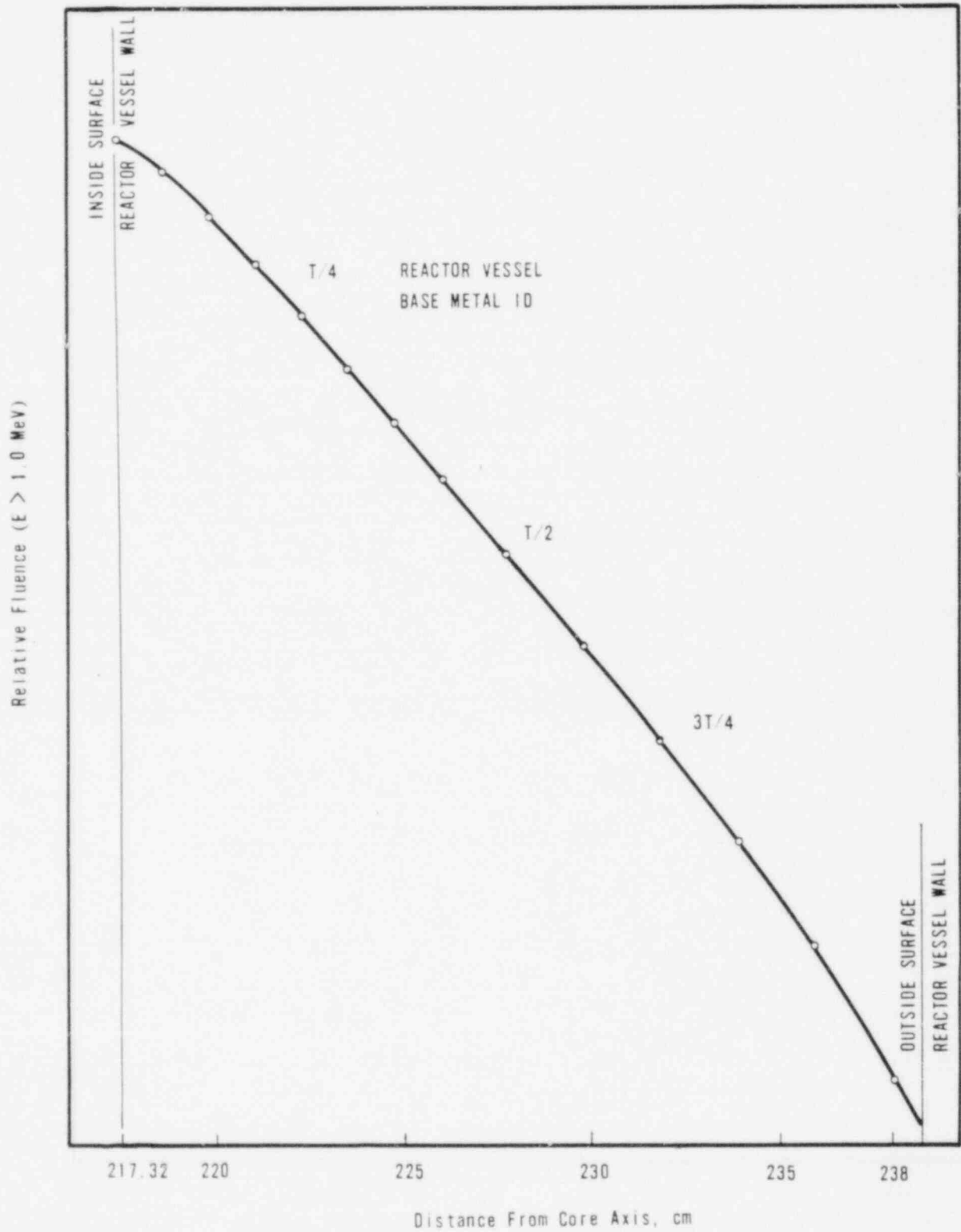
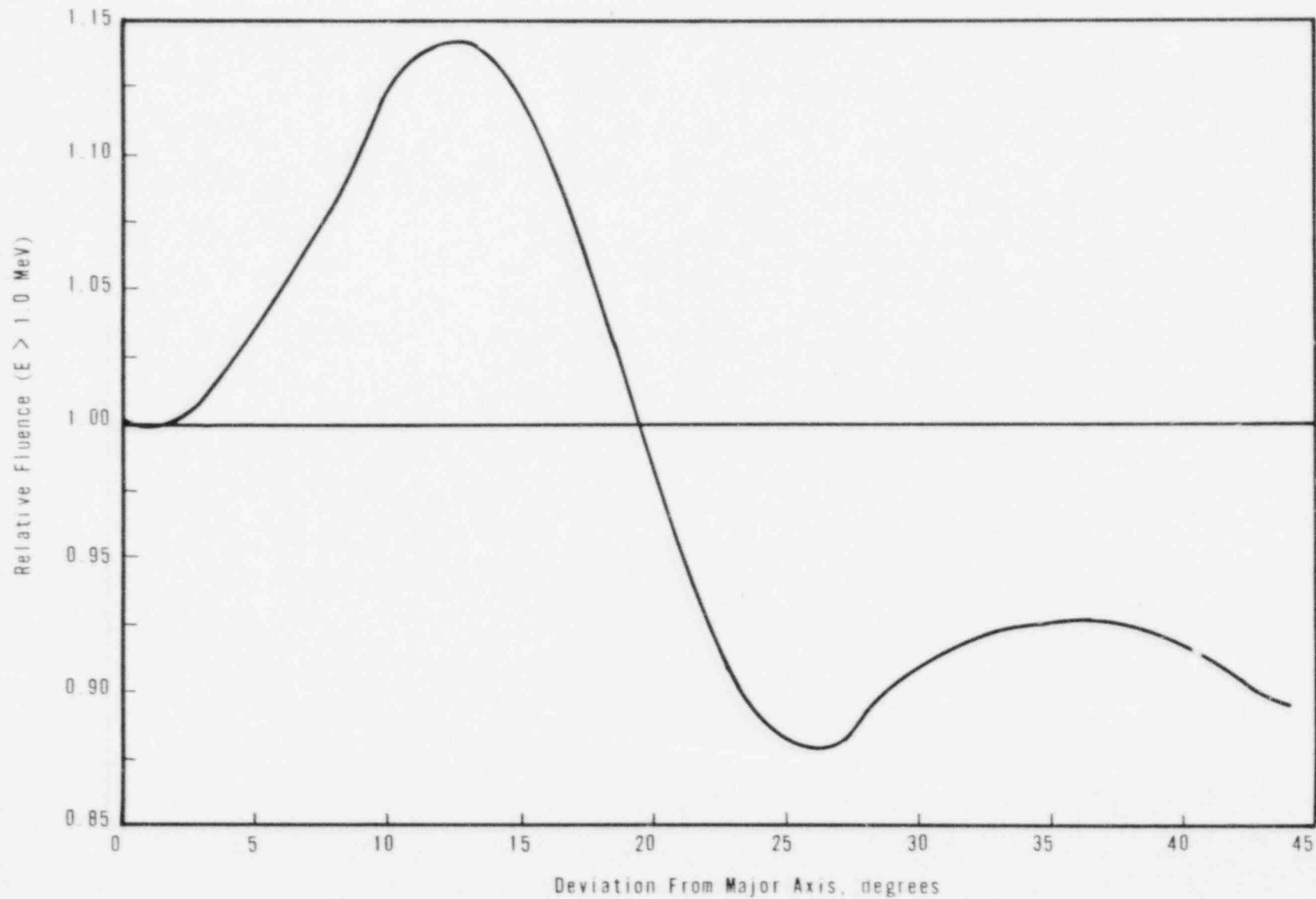


Figure 6-2. Azimuthal Fluence Gradient ($E > 1.0$ Mev) at Inside Surface of Oconee 2 Reactor Vessel, Cycles 2, 3, and 4



6-7

Babcock & Wilcox

7. DISCUSSION OF CAPSULE RESULTS

7.1. Preirradiation Property Data

A review of the unirradiated properties of the reactor vessel core belt region indicated no significant deviation from expected properties except in the case of the upper shelf properties of the weld metal. Based on the predicted end-of-service peak neutron fluence value at the 1/4T vessel wall location and the copper content of this weld, it is predicted that the end-of-service Charpy upper shelf energy (USE) will be below 50 ft-lb. This weld was selected for inclusion in the surveillance program in accordance with the criteria in effect at the time the program was designed for Oconee Unit 2. The applicable selection criterion was based on the unirradiated properties only.

7.2. Irradiated Property Data

7.2.1. Tensile Properties

Table 7-1 compares irradiated and unirradiated tensile properties. At both room temperature and elevated temperature, the ultimate and yield strength changes in the base metal due to irradiation and the corresponding changes in ductility are negligible. There appears to be some strengthening, as indicated by increases in ultimate and yield strength and similar decreases in ductility properties. All changes observed in the base metal are such as to be considered within acceptable limits. The changes in the properties of the weld metal at both room temperature and 580F are greater than those observed for the base metal, indicating the greater sensitivity of the base metal to irradiation damage. In either case, the changes in tensile properties are insignificant relative to the analysis of the reactor vessel materials at this period in service life.

7.2.2. Impact Properties

The behavior of the Charpy V-notch impact data is more significant than tensile properties to the calculation of reactor system operating limitations.

Table 7-2 compares the observed changes in irradiated Charpy impact properties to the predicted changes using Regulatory Guide 1.99, Revision 1.

The 50-ft-lb transition temperature shift for the base metal was in good agreement with the shift that would be predicted according to Regulatory Guide 1.99. The less-than-ideal comparison may be attributed to the spread in the data of the unirradiated material combined with the small number of data points to establish the irradiated curve. Under these conditions, the comparison indicates that the estimated curves in RG 1.99 for medium-copper materials and at low fluence levels are reasonably accurate and conservative for predicting the 50-ft-lb transition temperature shifts.

The 30-ft-lb transition temperature shift for the base metal does not agree as well with the value predicted according to RG 1.99, although these values are expected to exhibit better comparison when it is considered that a major portion of the data used to develop RG 1.99 was taken at the 30-ft-lb temperature.

The increase in the 35-mil lateral expansion transition temperature is compared with the shift in RT_{NDT} curve data in a manner similar to the comparison made for the 50-ft-lb transition temperature shift. These data show a behavior similar to that observed from the comparison of the observed and predicted 50-ft-lb transition data.

All the transition temperature measurements for the weld metal agree poorly with the predicted shift. This can be attributed to the chemistry of the weld metal compared to the nominal chemistry of normal weld metal for which the prediction curves were developed. The data do indicate that the prediction techniques produce conservative values for the predicted values of shift of the weld metal.

The data for the decrease in Charpy USE with irradiation showed a conservative agreement with predicted values for both the base and weld metals. However, a less-than-ideal comparison of the measured data and the predicted value would not be unexpected in view of the lack of data for medium- to high-copper-content materials at the low to medium fluence values that were used to develop the estimating curves.

Results from other capsules indicate that the RT_{NDT} estimating curves have greater inaccuracies at the very low neutron fluence levels ($\leq 1 \times 10^{18}$ n/cm²).

This inaccuracy is attributed to the limited data at the low fluence values and to the fact that the majority of the data used to define the curves in RG 1.99 are based on the shift at 30 ft-lb as compared to the current requirement of 50 ft-lb. For most materials, the shifts measured at 50 ft-lb/35 MLE are expected to be higher than those measured at 30 ft-lb. The significance of the shifts at 50 ft-lb and/or 35 MLE is not well understood at present, especially for materials having USE values that approach the 50-ft-lb level and/or the 35-MLE level. Materials with this characteristic may have to be evaluated at transition energy levels lower than 50 ft-lb.

The design curves for predicting the shift at 50 ft-lb/35 MLE will probably be modified as data become available. Until that time, the design curves for predicting the RT_{NDT} shift as given in RG 1.99 are considered adequate for predicting the RT_{NDT} shift of those materials for which data are not available and will continue to be used to establish the pressure-temperature operational limitations for the irradiated portions of the reactor vessel.

The less-than-ideal agreement of the change in Charpy USE is further support of the inaccuracy of the prediction curves at the lower fluence levels. Although the prediction curves are conservative in that they predict a larger drop in USE than is observed for a given fluence and copper content, the conservatism can unduly restrict operational limitations. These data support the contention that the USE drop curves will have to be modified as more reliable data become available; until that time the design curves used to predict the decrease in USE are conservative.

Table 7-1. Comparison of Tensile Test Results

	<u>Room temp test</u>		<u>Elevated temp test (580F)</u>	
	<u>Unirr</u>	<u>Irrad</u>	<u>Unirr</u>	<u>Irrad</u>
<u>Base Metal - AAW-163, Longitudinal</u>				
Fluence, 10^{18} n/cm ² (> 1 Mev)	0	3.37	0	3.37
Ult tensile strength, ksi	89.2	93.1	83.3	86.9
0.2% yield strength, ksi	68.0	71.4	61.5	64.7
Uniform elongation, %	11.1	14.1	9.5	13.6
Total elongation, %	28.1	28.8	29.8	24.9
RA, %	69.7	68.9	73.1	68.1
<u>Weld Metal - WF-209-1</u>				
Fluence, 10^{18} n/cm ² (> 1 Mev)	0	3.37	0	3.37
Ult tensile strength, ksi	95.2	110.6	89.7	102.2
0.2% yield strength, ksi	81.4	97.8	69.8	86.3
Uniform elongation, %	10.7	15.1	10.4	12.1
Total elongation, %	25.6	21.0	20.6	20.4
RA, %	57.9	43.4	48.9	43.9

Table 7-2. Observed Vs Predicted Changes in Irradiated Charpy Impact Properties

<u>Material</u>	<u>Observed</u>	<u>Predicted</u> ^(a)
<u>Increase in 30-ft-lb trans temp, F</u>		
Base material (AAW-163)		
Transverse	17	25
Longitudinal	Neg.	--
Heat-affected zone (AAW-163)	--	--
Weld metal (WF-209-1)	114	186
Correlation, HSST plate 02	71	90
<u>Increase in 50-ft-lb trans temp, F</u>		
Base material (AAW-163)		
Transverse	20	25
Longitudinal	Neg.	--
Heat-affected zone (AAW-163)	--	--
Weld metal (WF-209-1)	Ind.	186
Correlation, HSST plate 02	53	90
<u>Increase in 35-MLE trans temp, F</u>		
Base material (AAW-163)		
Transverse	18	25 ^(b)
Longitudinal	0	--
Heat-affected zone (AAW-163)	--	--
Weld metal (WF-209-1)	84	186 ^(b)
Correlation, HSST plate 02	69	90 ^(b)
<u>Decrease in Charpy USE, ft-lb</u>		
Base material (AAW-163)		
Transverse	--	--
Longitudinal	17	23
Heat-affected zone (AAW-163)	4	23
Weld metal (WF-209-1)	19	24
Correlation, HSST plate 02	27	25

(a) These values predicted per RG 1.99, Revision 1.

(b) Based on the assumption that MLE, as well as 50-ft-lb transition temperature, is used to control the shift in RT_{NDT} .

8. DETERMINATION OF RCPB PRESSURE-TEMPERATURE LIMITS

The pressure-temperature limits of the reactor coolant pressure boundary (RCPB) (RCPB) of Oconee Unit 2 are established in accordance with the requirements of 10 CFR 50, Appendix G. The methods and criteria employed to establish operating pressure and temperature limits are described in topical report BAW-10046P.⁴ The objective of these limits is to prevent nonductile failure during any normal operating condition, including anticipated operation occurrences and system hydrostatic tests. The loading conditions of interest include the following:

1. Normal operations, including heatup and cooldown.
2. Inservice leak and hydrostatic tests.
3. Reactor core operation.

The major components of the RCPB have been analyzed in accordance with 10 CFR 50, Appendix G. The closure head region, the reactor vessel outlet nozzle, and the beltline region have been identified as the only regions of the reactor vessel (and consequently of the RCPB) that regulate the pressure-temperature limits. Since the closure head region is significantly stressed at relatively low temperatures (due to mechanical loads resulting from bolt preload), this region largely controls the pressure-temperature limits for the first several service periods. The reactor vessel outlet nozzle also affects the pressure-temperature limit curves of the first several service periods. This is due to the high local stresses at the inside corner of the nozzle, which can be two to three times the membrane stresses of the shell. After the first several years of neutron radiation exposure, the RT_{NDT} of the beltline region materials will be high enough that the beltline region of the reactor vessel will start to control the pressure-temperature limits of the RCPB. For the service period for which the limit curves are established, the maximum allowable pressure as a function of fluid temperature is obtained through a point-by-point comparison of the limits imposed by the closure head region, the outlet nozzle, and the beltline region. The maximum allowable pressure is taken to be the lowest of three calculated pressures.

The limit curves for Oconee Unit 2 are based on the predicted values of the adjusted reference temperatures of all the beltline region materials at the end of the fifteenth full-power year. This year was selected because it is estimated that the third surveillance capsule will be withdrawn at the end of the refueling cycle when the estimated fluence corresponds to approximately the eighteenth full-power year. The time difference between the withdrawal of the second and third surveillance capsules provides enough time to re-establish the operating pressure and temperature limits for the period of operation beyond the fifteenth full-power year.

The unirradiated impact properties were determined for the surveillance beltline region materials in accordance with 10 CFR 50, Appendixes G and H. For the other beltline region and RCPB materials for which the measured properties are not available, the unirradiated impact properties and residual elements (as originally established for the beltline region materials) are listed in Table A-1. The adjusted reference temperatures are calculated by adding the predicted radiation-induced ΔRT_{NDT} and the unirradiated RT_{NDT} . The predicted ΔRT_{NDT} is calculated using the respective neutron fluence and copper and phosphorus contents. Figure 8-1 illustrates the calculated peak neutron fluence at several locations through the reactor vessel beltline region wall as a function of exposure time. The supporting information for Figure 8-1 is described in section 6. The neutron fluence values of Figure 8-1 are the predicted fluences, which have been demonstrated (section 6) to be conservative. The design curves of Regulatory Guide 1.99* were used to predict the radiation-induced ΔRT_{NDT} values as a function of the material's copper and phosphorus contents and neutron fluence.

The neutron fluences and adjusted RT_{NDT} values of the beltline region materials at the end of the fifteenth full-power year are listed in Table 8-1. The neutron fluences and adjusted RT_{NDT} values are given for the 1/4T and 3/4T vessel wall locations (T = wall thickness). The assumed RT_{NDT} of the closure head region and the outlet nozzle steel forgings is 60F, in accordance with BAW-10046P.⁴

- - - - -
*Revision 1, January 1976.

Figure 8-2 is the reactor vessel pressure-temperature limit curve for normal heatup. This figure also shows the core criticality limits as required by 10 CFR 50, Appendix C. Figures 8-3 and 8-4 show the vessel pressure-temperature limit curve for normal cooldown and for heatup during inservice leak and hydrostatic tests, respectively. All pressure-temperature limit curves are applicable up to the sixteenth EFPY. Protection against nonductile failure is ensured by maintaining the coolant pressure below the upper limits of the pressure-temperature limit curves. The acceptable pressure and temperature combinations for reactor vessel operation are below and to the right of the limit curve. The reactor is not permitted to go critical until the pressure-temperature combinations are to the right of the criticality limit curve. To establish the pressure-temperature limits for protection against nonductile failure of the RCPB, the limits presented in Figures 8-2 through 8-4 must be adjusted by the pressure differential between the point of system pressure measurement and the pressure on the reactor vessel controlling the limit curves. This is necessary because the reactor vessel is the most limiting component of the RCPB.

Table 8-1. Data for Preparation of Pressure-Temperature Limit Curves for
Oconee Unit 2 - Applicable Through 15 EFPY

Material Ident		Beltline region location	Weldment location			Unirr RT NDT* F	Chemistry		Neutron fluence at end of 15 EFPY (E = 1 Mev), n/cm ²		Radiation-induced ΔRT _{NDT} at end of 15 EFPY, °F(*)		Adjusted RT _{NDT} at end of 15 EFPY, °F	
Heat No.	Type		Core midplane to weld Cl., cm	Location from major axis, degrees	Weld 1/4T location		Co content, %	P content, %	At 1/4T	At 3/4T	At 1/4T	At 3/4T	At 1/4T	At 3/4T
AM4-27	SA508, Cl 2	Lower nozzle belt	--	--	--	(60)	0.06	0.006	2.43E18	5.55E17	20	9	80	69
AAW-163	SA508, Cl 2	Upper shell	--	--	--	20	0.04	0.006	3.20E18	7.30E17	23	11	43	31
AAW-164	SA508, Cl 2	Lower shell	--	--	--	-10	0.02	0.010	3.20E18	7.30E17	28	13	18	3
WF-154	Weld	Upper circum. seam	123	--	Yes	(20)	(-)	(-)	2.43E18	5.55E17	145	69	165	89
WF-25	Weld	Mid-circum. seam	-63	--	Yes	-14	(-)	(-)	3.20E18	7.30E17	195	93	181	29
WF-112	Weld	Lower circum. seam	-249	--	Yes	0	(-)	(-)	1.79E16	4.09E15	13	4	13	4

Notes: () : estimated per BAW-10046P.¹

(-): per BAW-1511P, October 1980.

(*): per Regulatory Guide 1.99, Revision 1.

Figure 8-1. Predicted Fast Neutron Fluences at Various Locations Through Reactor Vessel Wall for First 15 EFY

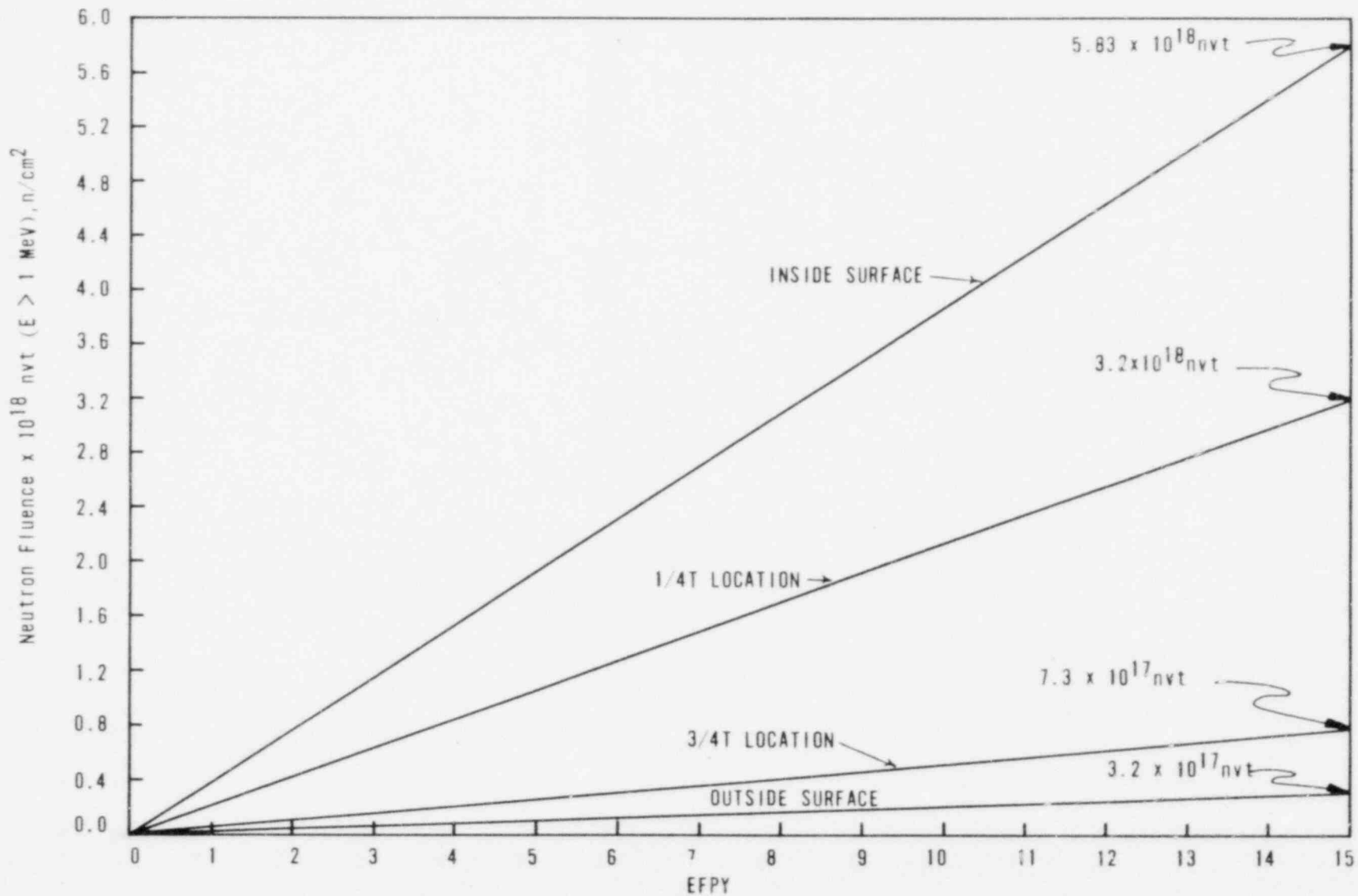


Figure 8-2. Reactor Vessel Pressure-Temperature Limit Curves for Normal Operation Heatup, Applicable for First 15 EFPY

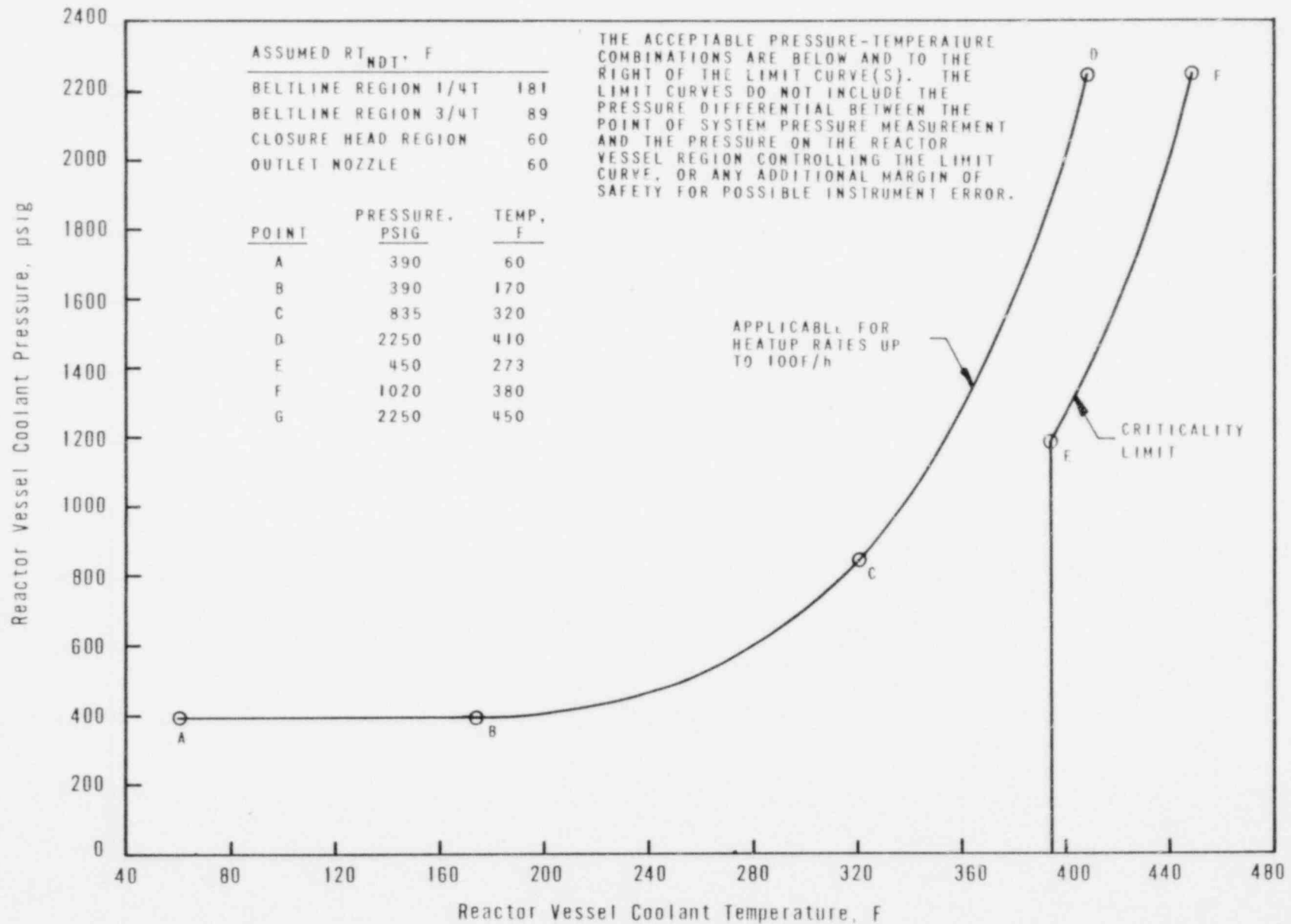


Figure 8-3. Reactor Vessel Pressure-Temperature Limit Curve for Normal Operation - Cooldown, Applicable for First 15 EFPY

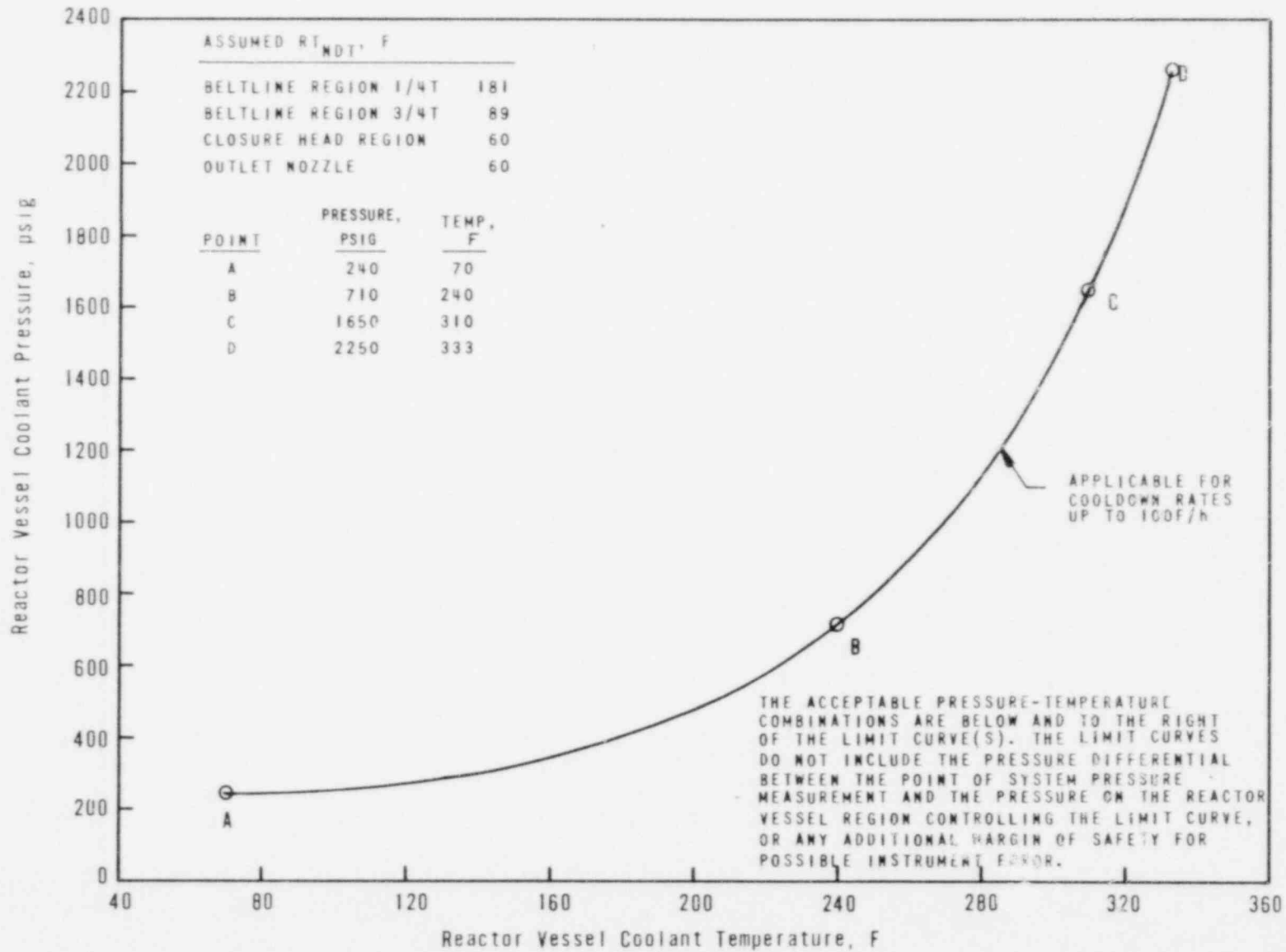
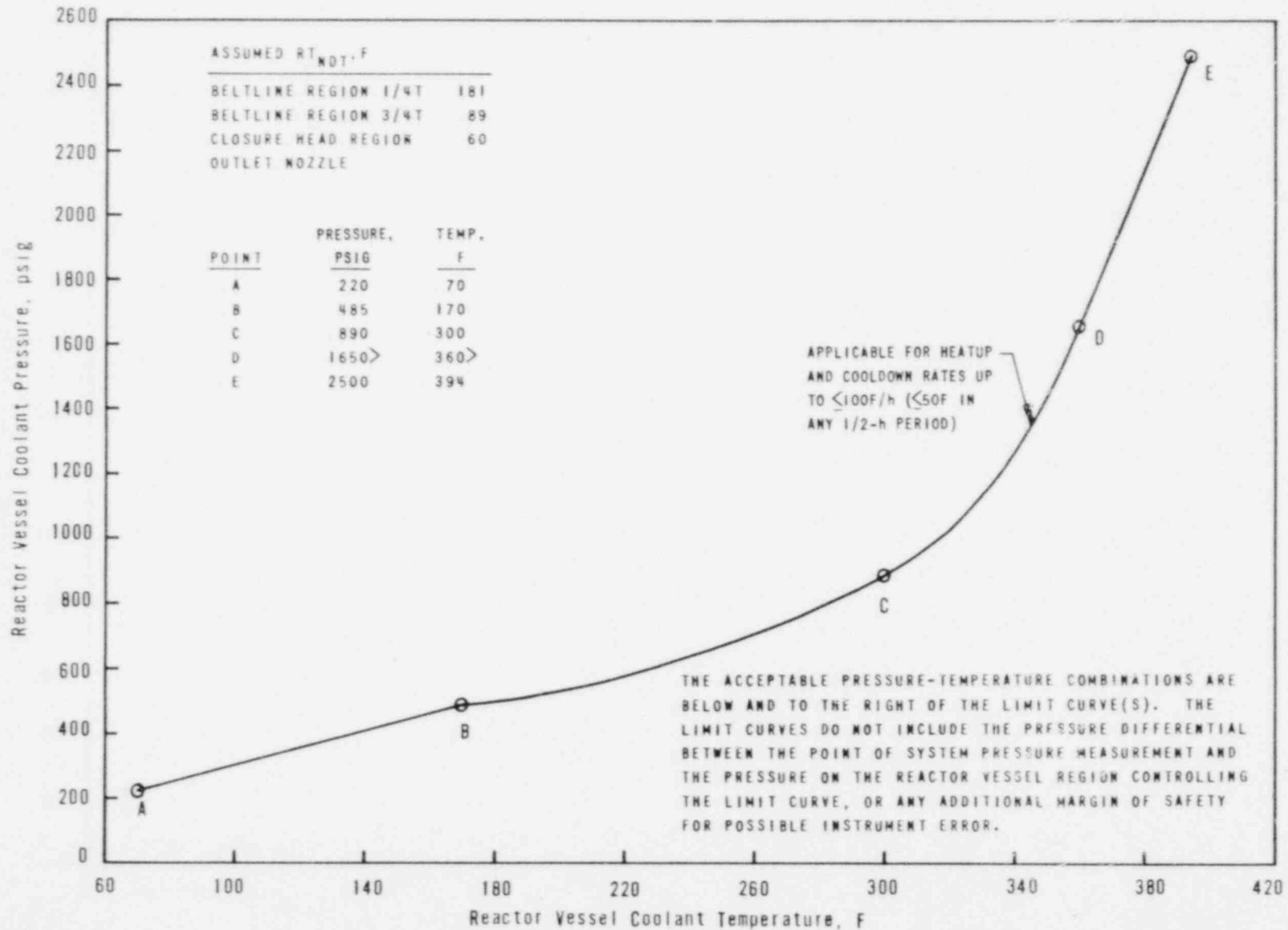


Figure 8-4. Reactor Vessel Pressure-Temperature Limit Curve for Inservice Leak and Hydrostatic Tests, Applicable for First 15 EFPY



9. SUMMARY OF RESULTS

The analysis of the reactor vessel material contained in OCII-A, the second surveillance capsule of the Oconee Unit 2 pressure vessel surveillance program, led to the following conclusions:

1. The capsule received an average fast fluence of 3.37×10^{18} n/cm² (E > 1 Mev). The predicted fast fluence for the reactor vessel T/4 location at the end of cycle 4 (1361 EFPD) is 9.8×10^{17} n/cm² (E > 1 Mev).
2. The fast fluence of 3.37×10^{18} n/cm² (E > 1 Mev) increased the RT_{NDT} of the capsule reactor vessel core region shell materials a maximum of 114F.
3. Based on a comparison of the fast flux in the surveillance capsule to that at the vessel wall and an 80% load factor, the calculated projected maximum fast fluence that the Oconee Unit 2 reactor pressure vessel will receive in 40 calendar years of operation is 1.20×10^{19} n/cm² (E > 1 Mev).
4. The increase in the RT_{NDT} for the base plate material agreed acceptably with that predicted by the currently used design curves of ΔRT_{NDT} versus fluence and demonstrated that the prediction techniques are conservative.
5. The increase in the RT_{NDT} for the weld metal did not agree well with that predicted by the currently used design curves of ΔRT_{NDT} versus fluence because the decrease in upper shelf energy distorted the measured shifts.
6. The current techniques used for predicting the change in Charpy impact upper shelf properties due to irradiation are conservative.
7. The analysis of the neutron dosimeters demonstrated that the analytical techniques used to predict the neutron flux and fluence were accurate.
8. The thermal monitors indicated that the capsule design was satisfactory for maintaining the specimens within the desired temperature range.

10. SURVEILLANCE CAPSULE REMOVAL SCHEDULE

Based on the postirradiation test results of capsule OCII-A, the following schedule is recommended for examination of the remaining capsules in the Oconee 2 reactor vessel surveillance program:

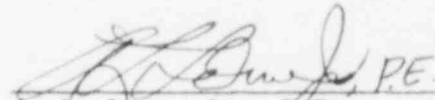
Capsule	Evaluation schedule		Est date ^(a) data available
	Est capsule fluence, n/cm ²	Estimated EFPY Surface 1/4T	
OCII-B	1.2×10^{19}	18 32	1987
OCII-E ^(b)	2.2×10^{19}	33 59	1987
OCII-D	Standby	-- --	--
OCII-F	Standby	-- --	--

(a) These dates do not represent the earliest dates that data will be available for the materials that control the operating limitations. Similar materials are included as part of the B&W Integrated Reactor Surveillance Program, which will provide necessary data on a timely basis.

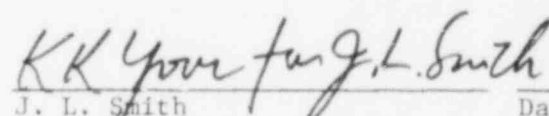
(b) Capsule contains weld metal specimens.

11. CERTIFICATION

The specimens were tested, and the data obtained from Oconee Nuclear Station, Unit 2 surveillance capsule OCII-A were evaluated using accepted techniques and established standard methods and procedures in accordance with the requirements of 10 CFR 50, Appendixes G and H.


A. L. Lowe, Jr., P.E. 4 Dec 1981
Project Technical Manager Date

This report has been reviewed for technical content and accuracy.


J. L. Smith 12-4-81
Component Engineering Date

APPENDIX A

Reactor Vessel Surveillance Program -
Background Data and Information

1. Material Selection Data

The data used to select the materials for the specimens in the surveillance program, in accordance with E-185-66, are shown in Table A-1. The locations of these materials within the reactor vessel are shown in Figure A-1.

2. Definition of Beltline Region

The beltline region of Oconee Nuclear Station, Unit 2 was defined in accordance with the data given in BAW-10100A.⁵

3. Capsule Identification

The capsules used in the Oconee 2 surveillance program are identified below by number and type.

Capsule Cross Reference Data

<u>ID No.</u>	<u>Type</u>
OCII-A	I
OCII-B	II
OCII-C	I
OCII-D	II
OCII-E	I
OCII-F	II

4. Specimens per Surveillance Capsule

See Tables A-2 and A-3.

Table A-1. Surveillance Program Material Selection Data for Oconee 2

Material ident.		Beltline region location	Core midplane to weld CL, cm	Drop weight T _{NDT} , F	Charpy data, C _{VN}				RT _{NDT} , F	Chemistry, %			
Heat No.	Type				Longitudinal @ 10F, ft-lb	Transverse				Cu	P	S	NI
					50 ft-lb	35 MLE	USE						
AMX 77	SA508 C1 2	Lower nozzle belt	--	--	90, 121, 106 103, 91, 128	--	--	--	--	0.06	0.006	0.009	0.74
AAW 163	SA508 C1 2	Upper shell	--	20	62, 77, 40	--	--	--	--	0.04	0.006	0.012	0.78
AWC 164	SA508 C1 2	Lower shell	--	20	82, 83, 90	--	--	--	--	0.02	0.010	0.010	0.78
WF-154	Weld	Circum seam	123	--	41, 37, 43	--	--	--	--	0.20	0.015	0.021	0.59
WF-25	Weld	Circum seam	-63	--	38, 28, 49	--	--	--	--	0.29	0.019	0.010	0.71
WF-112	Weld	Circum seam	-249	--	35, 40, 30	--	--	--	--	0.22	0.024	0.006	0.58
WF-209-1A	Weld	Surv. weld	--	--	29, 30, 32	--	--	--	--	0.34	0.013	0.010	0.68

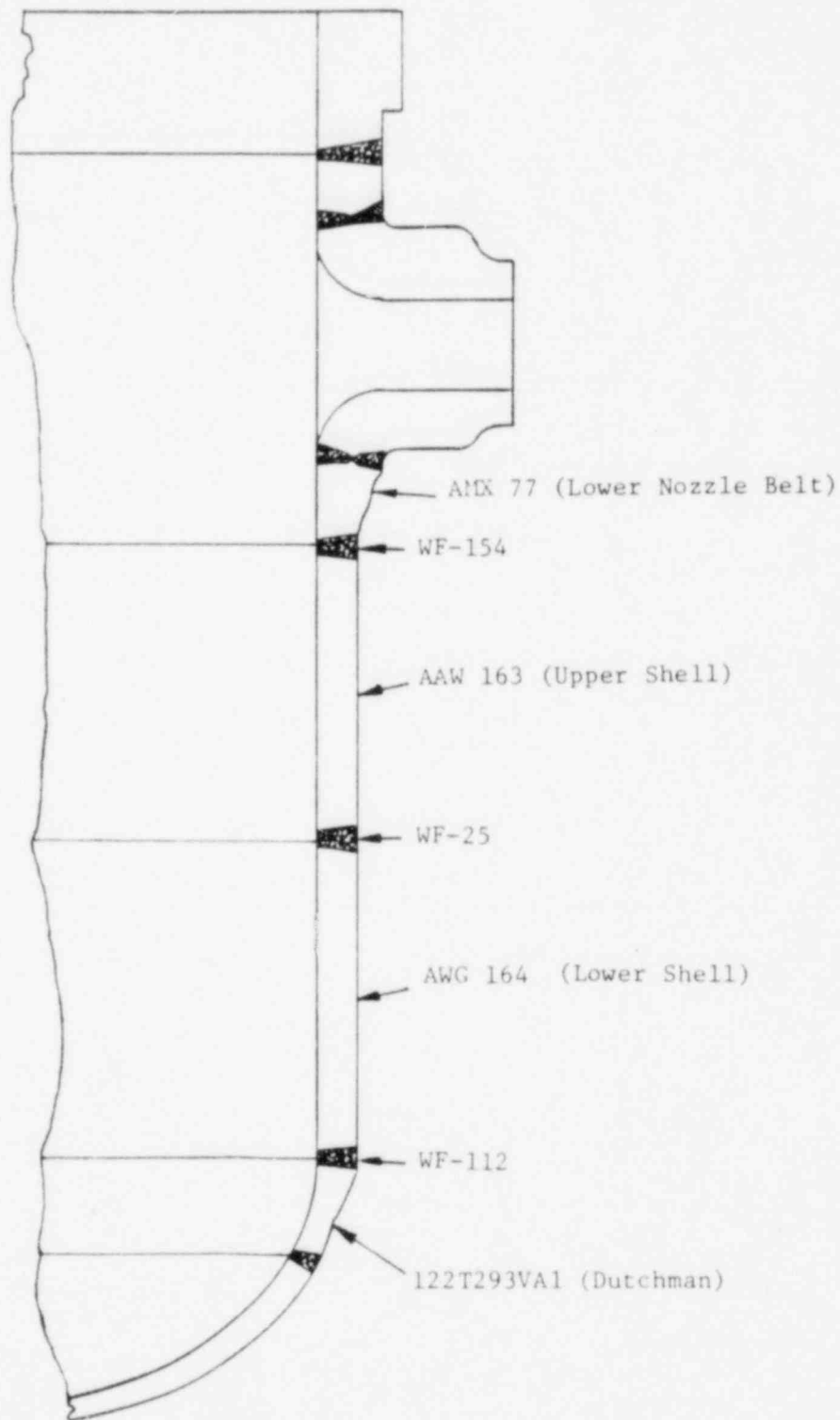
Table A-2. Materials and Specimens in Upper Surveillance Capsules OCII-A, OCII-C, and OCII-E

<u>Material description</u>	<u>No. of specimens</u>	
	<u>Tensile</u>	<u>Charpy</u>
Weld metal, WF-209-1A	4	8
HAZ A, heat AAW-163, longitudinal	0	8
Base metal material, plate A, heat AAW-163		
Longitudinal	4	8
Transverse	0	4
Correlation, HSST plate 02	<u>0</u>	<u>8</u>
Total per capsule	8	36

Table A-3. Materials and Specimens in Lower Surveillance Capsules OCII-B, OCII-D, and OCII-F

<u>Material description</u>	<u>No. of specimens</u>	
	<u>Tensile</u>	<u>Charpy</u>
HAZ B, heat AWG-164, longitudinal	4	10
Base metal material, plate B, heat AWG-164		
Longitudinal	4	10
Transverse	0	8
Correlation, HSST plate 02	<u>0</u>	<u>8</u>
Total per capsule	8	36

Figure A-1. Location and Identification of Materials Used in Fabrication of Reactor Pressure Vessel



APPENDIX B
Preirradiation Tensile Data

Table B-1. Preirradiation Tensile Properties of Shell
Plate Material, Heat AAW 163

Specimen No.	Test temp, F	Strength, psi		Elongation, %		Red'n of area, %
		Yield	Ult.	Unif.	Total	
<u>Longitudinal</u>						
EE-701	RT	70,420	90,680	10.74	27.14	69.3
706	RT	66,790	88,550	11.83	29.28	68.5
709	RT	66,690	88,300	10.88	27.86	71.2
Mean	RT	67,970	89,180	11.15	28.09	69.67
Std dev'n		1,740	300	0.48	0.89	1.13
EE-704	580	61,580	82,110	9.48	30.7	74.8
707	580	62,460	82,110	9.59	30.0	75.7
718	580	60,490	85,630	9.52	28.6	68.8
Mean	580	61,510	83,280	9.53	29.77	73.1
Std dev'n	±5	810	1,660	0.05	0.87	3.06

Table B-2. Preirradiation Tensile Properties of Weld
Metal - Longitudinal, WF-209-1

Specimen No.	Test temp, F	Strength, psi		Elongation, %		Red'n of area, %
		Yield	Ult.	Unif.	Total	
EE-102	RT	81,190	95,140	10.84	26.1	60.7
105	RT	83,530	96,640	10.36	24.6	51.0
120	RT	79,430	93,800	11.0	26.1	62.1
Mean	RT	81,380	95,190	10.73	25.6	57.94
Std dev'n		1,680	1,160	0.27	0.71	4.94
EE-113	580	69,170	89,210	10.4	20.7	46.8
118	580	69,730	89,910	10.4	20.7	49.9
119	580	70,610	90,000	10.25	20.4	50.0
Mean	580	69,840	89,710	10.35	20.6	48.9
Std dev'n	±5	596	356	0.07	0.14	1.49

APPENDIX C
Preirradiation Charpy Impact Data

Table C-1. Preirradiation Charpy Impact Data for Shell Course Material - Longitudinal Orientation, Heat AAW 163

Specimen No.	Test temp, F	Absorbed energy, ft-lb	Lateral expansion, 10^{-3} in.	Shear fracture, %
EE-727	361.7	140	63.5	100
720	361.4	134	68	100
732	359.5	132	71	100
EE-750	280.9	151	65	100
742	280.4	145	69.5	100
745	280.3	145	74.5	100
EE-734	200.9	150.5	68	100
706	200.5	154	71	100
702	200.4	147	74	100
EE-748	141	146	69.5	100
741	140.8	156	68.5	100
746	140.5	153	70.5	100
EE-719	80.2	108	67.5	45
736	80	122	68.5	65
712	79.9	98	64	35
EE-752	21.3	83	64.5	25
747	20.9	81	62.5	12
751	20.8	82	65.5	20
EE-735	0.1	55	40	1
701	0.1	47.5	35.5	--
730	-0.6	60	44.5	--
EE-744	11.8	75	54	6
743	-12.4	79	57	8
749	-13.9	16	12.5	<1
EE-705	-40.9	13	9	0
716	-41.1	23	16	0
729	-41.6	27	20	0

Table C-2. Preirradiation Charpy Impact Data for Shell Course Material - Transverse Orientation, Heat AAW 163

Specimen No.	Test temp, F	Absorbed energy, ft-lb	Lateral expansion, 10^{-3} in.	Shear fracture, %
EE-626	361.3	122	74	100
625	361.1	121	68	100
615	359.3	124	75	100
620	358.7	122	70.5	100
EE-630	279.4	127	71	100
632	278.8	118	68	100
637	278.3	122	69	100
EE-618	202	124	73	100
606	201	128	69.5	100
627	197.4	147	70.5	100
EE-639	141.1	134	73.5	100
633	140.5	119	63.5	92
640	139	128	70.5	100
EE-619	79.9	119	60.5	100
608	79.8	109	65	65
607	79.8	117	67	80
EE-629	20.5	62	50.5	8
631	20.4	77	60	25
EE-610	9.9	65	50	1
625	0.5	49	39	1
616	-1.5	61	44	0
EE-635	-15	54	40	4
634	-15.5	39	28	2
638	-18	38	31	2
EE-605	-38.9	32	24.5	1
603	-39	24	17	0
622	-41.1	18	14	0

Table C-3. Preirradiation Charpy Impact Data for Shell Course Material - HAZ, Longitudinal Orientation, Heat AAW 163

Specimen No.	Test temp, F	Absorbed energy, ft-lb	Lateral expansion, 10 ⁻³ in.	Shear fracture, %
EE-434	361.8	164	68	100
418	360.8	174	67.5	100
411	360.3	131	76.5	100
EE-444	281.6	113	74	100
449	280.6	104	74	100
442	280	145	65	100
EE-407	202	124	57.5	100
425	200.5	86	49	100
435	199.5	185	73.5	100
EE-451	140.9	148	75.5	100
446	139	132	75	100
441	138.9	129	69.5	100
EE-437	80.6	81	43.5	100
421	80.5	134	73.5	75
402	80.3	158	73	100
EE-443	41.9	112	62.5	45
448	41.1	101	62	35
450	41.8	75	54.5	40
EE-438	0.6	97	56	20
418	0.5	128.5	68	40
406	0	114	57	45
EE-447	-39.7	81	53	12
452	-40.0	57	37	3
445	-40.1	53	36.5	8
EE-422	-79.7	90	49	35
426	-80.6	100	58.5	20
423	-82.5	73	39.5	5

Table C-4. Preirradiation Charpy Impact Data for Weld Metal, WF-209-1

Specimen No.	Test temp, F	Absorbed energy, ft-lb	Lateral expansion, 10^{-3} in.	Shear fracture, %
EE-014	361	67	53.5	100
032	360.8	72	52.5	100
035	360.1	65	49	100
EE-019	202.5	63	49.5	100
036	201.4	67.5	45	100
016	198.2	64	46	100
EE-020	120.9	68	47	98
011	120.3	66	47	100
006	120.3	66	44	100
EE-031	80.9	60	42.5	75
015	80.2	60	42	80
012	80.2	55	32	60
EE-024	0.5	27	25.5	25
022	-0.5	31	28.5	20
008	-0.5	25	23	15

Figure C-1. Impact Data From Unirradiated Base Metal (AAW-163) HAZ, Longitudinal Orientation

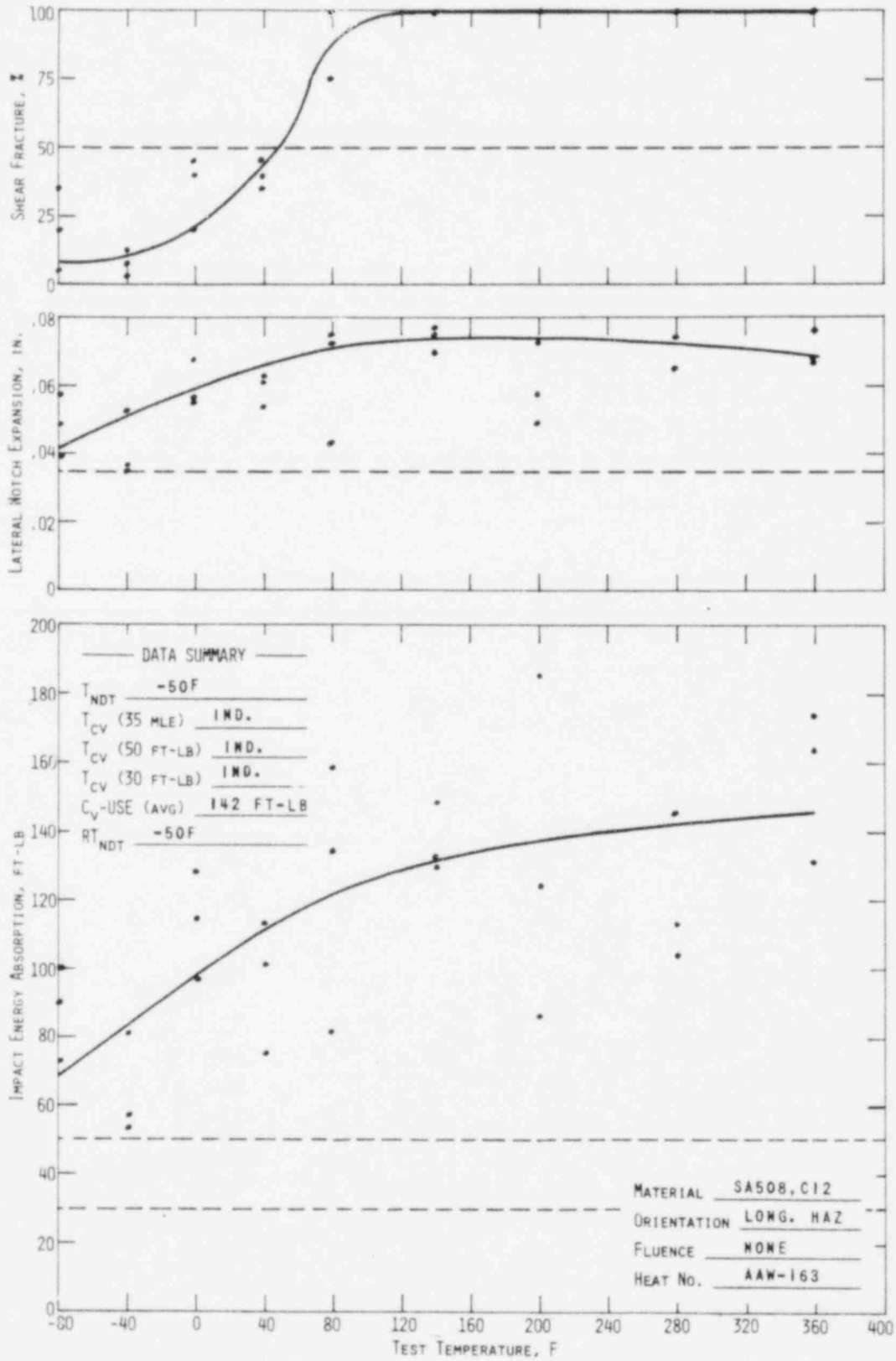


Figure C-2. Impact Data From Unirradiated Base Metal (AAW-163), Transverse Orientation

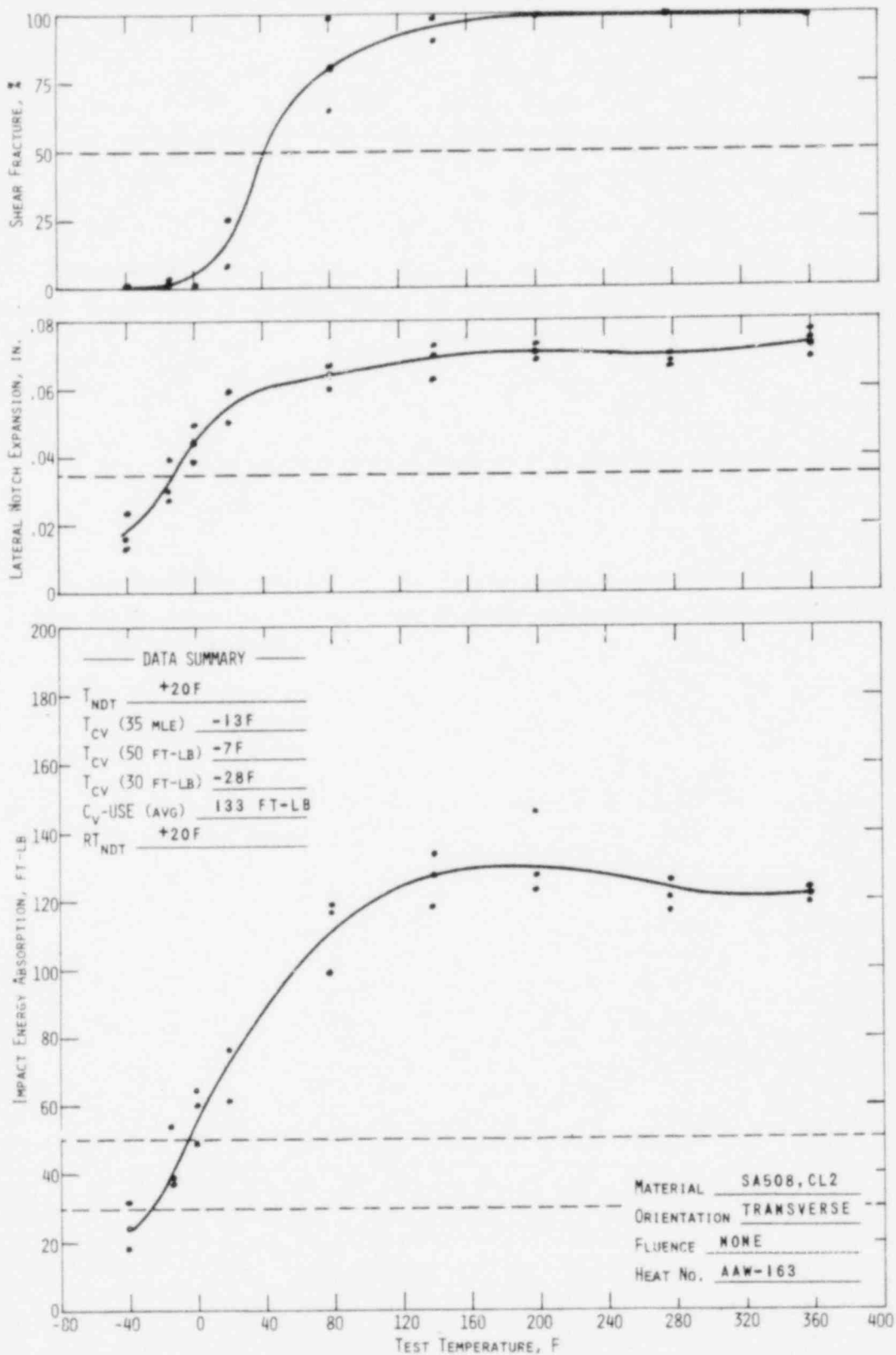


Figure C-3. Impact Data From Unirradiated Base Metal (AAW-163), Longitudinal Orientation

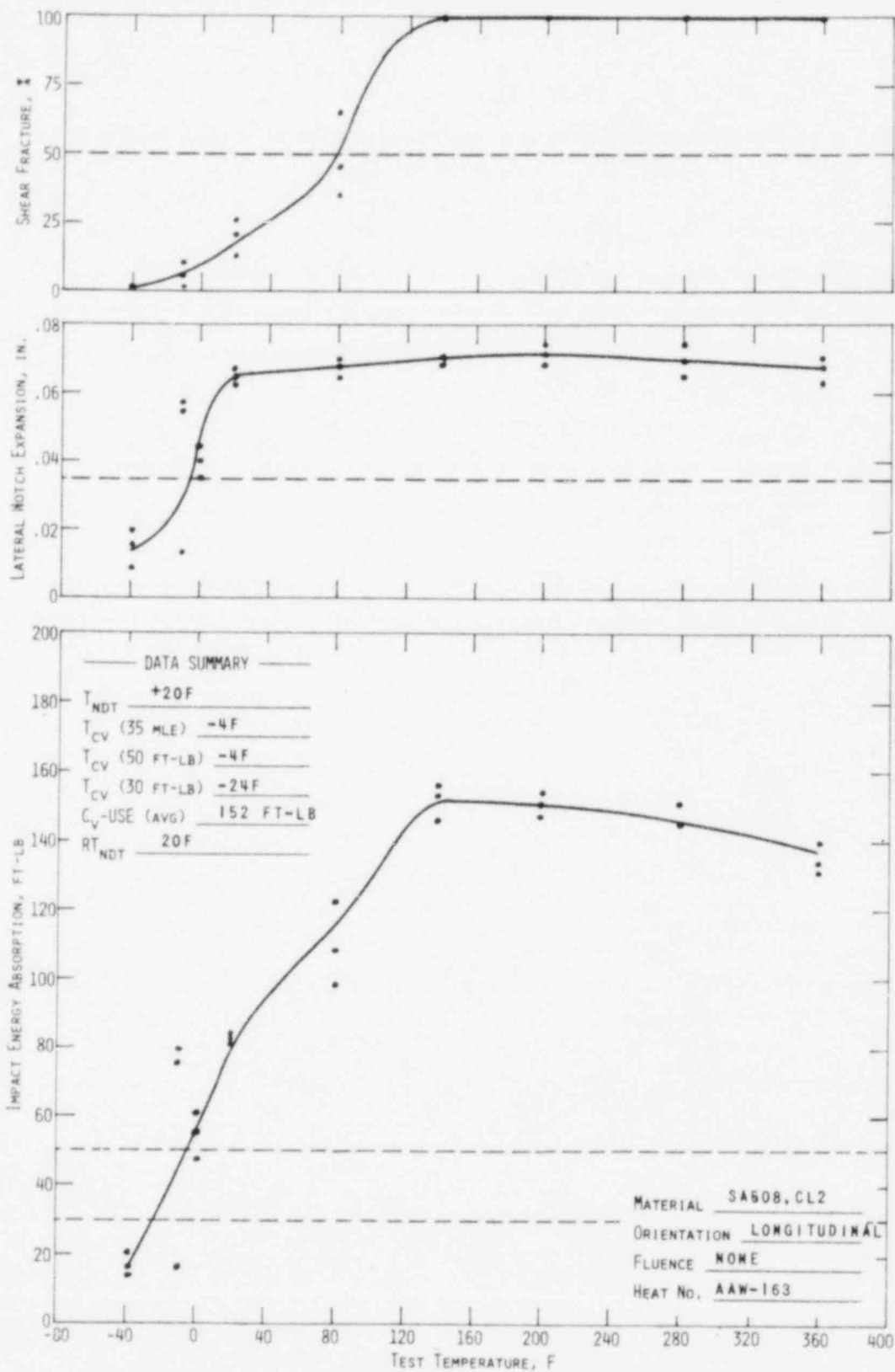
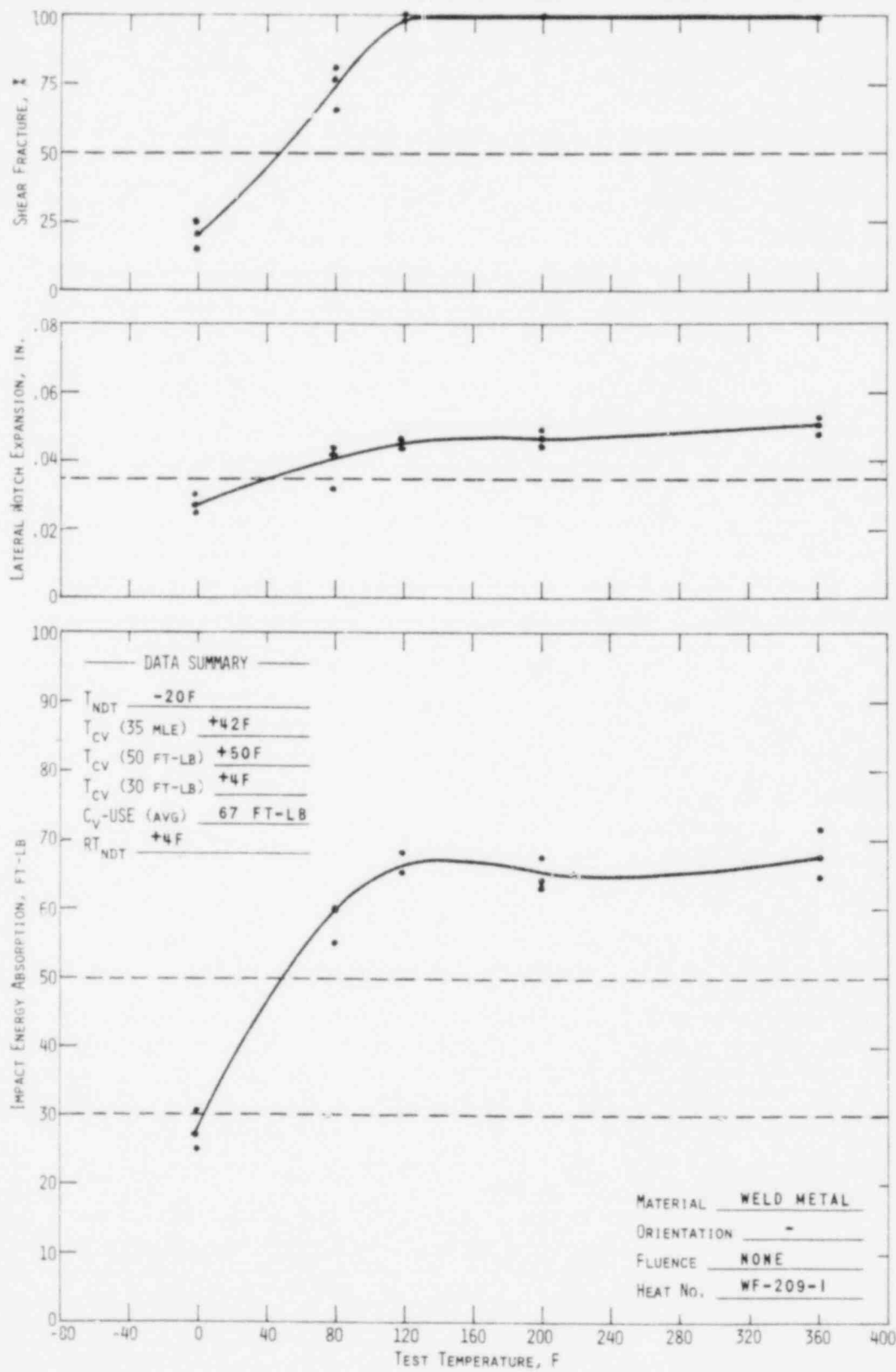


Figure C-4. Impact Data From Unirradiated Weld Metal



APPENDIX D
Fluence Analysis Procedures

1. Analytical Method

Energy-dependent neutron fluxes at the detector locations were determined by a discrete ordinates solution of the Boltzmann transport equation with the two-dimensional code DOT3.5.⁵ The Oconee 2 and CR-3 reactors were modeled from the core out to the primary concrete shield in R-theta geometry [based on a plan view along the core midplane and one-eighth core symmetry in the azimuthal (theta) dimension]. Also included was an explicit model of a surveillance capsule assembly in the downcomer region. The reactor model contained the following regions: core, liner, bypass coolant, core barrel, inlet coolant, thermal shield, inlet coolant (downcomer), pressure vessel, cavity, and concrete shield. Input data to the code included a pin-by-pin, time-averaged power distribution, CASK23E 22-group microscopic neutron cross sections⁷, S_8 order of angular quadrature, and P_3 expansion of the scattering cross section matrix. Reactor conditions — power distribution, temperature, and pressure — were averaged over the irradiation period. A more detailed description of the calculational procedure (except for capsule modeling) is presented in reference 8.

Because of computer storage limitations, two geometric models were required to cover the distance from the core to the primary shield. A boundary source output from model A (core to downcomer region) was used as input to model B (thermal shield to primary shield), which included the capsule assembly. In those cases where the capsule "shadowed" the maximum flux location in the pressure vessel, a model C (model B without a capsule assembly) was used to obtain vessel flux unperturbed by the presence of a capsule. For a reactor without surveillance capsules, an additional model A and model C were calculated. In this way the effect of the specific power distribution in that reactor on vessel fluence was accounted for. Thus, two sets of calculations were required — one to determine capsule fluence, which was based on Oconee 2 and CR-3 operating conditions, and a second set to determine vessel fluence, which was based on Oconee 2 operating conditions for cycles 2 through 4.

Flux output from the DOT3.5 calculations required only an axial distribution correction to provide absolute values.⁶ An axial shape factor (local:average axial flux ratio) was obtained from fuel burnup distributions in the peripheral fuel assemblies nearest the capsule location. This procedure assumes that the axial fast flux shape in the capsule and the pressure vessel is the same as the axial power distribution in the closest fuel assembly. This is considered

to be a conservative assumption in 177-FA reactor geometry because the axial shape should tend to flatten as distance from the core increases. This factor was 1.10 averaged over an elevation corresponding to the capsule length in CR-3 and applied to the surveillance capsule; a maximum value of 1.17 was applied to the pressure vessel in Oconee 2.

The calculation described above for CR-3 provides the neutron flux as a function of energy at the capsule position. These calculated data are used in the following equations to obtain the activities used for comparison with the experimental values. The equation for the calculated activity D (in $\mu\text{Ci/g}$) is as follows:

$$D_i = \frac{N}{A_n} \frac{1}{3.7 \times 10^{10}} f_i \int_E \sigma_n(E) \phi(E) \sum_{j=1}^M F_j (1 - e^{-\lambda_i t_j}) e^{-\lambda_i (T - \tau_j)} \quad (\text{D-1})$$

where

- N = Avogadro's number,
- A_n = atomic weight of target material n,
- f_i = either weight fraction of target isotope in nth material or fission yield of desired isotope,
- $\sigma_n(E)$ = group-averaged cross sections for material n (listed in Table E-3),
- $\phi(E)$ = group-averaged fluxes calculated by DOT3.5 analysis⁶,
- F_j = fraction of full power during jth time interval, t_j ,
- λ_i = decay constant of ith material,
- t_j = interval of power history,
- T = sum of total irradiation time, i.e., residual time in reactor, and wait time between reactor shutdown and counting,
- τ_j = cumulative time from reactor startup to end of jth time period, i.e., $\tau_j = \sum_{k=1}^j t_k$.

The normalizing constant C is obtained from the ratio of measured to calculated activities:

$$C = \frac{D_i \text{ (measured)}}{D_i \text{ (calculated)}} \quad (\text{D-2})$$

With C specified, the neutron fluence greater than 1 Mev can be calculated from

$$\phi(E > 1.0 \text{ Mev}) = C \sum_{E=1}^{15 \text{ Mev}} \phi(E) \sum_{j=1}^M F_j t_j \quad (D-3)$$

where M is the number of irradiation time intervals; the other values are defined above. The normalization constant for the OCII-A capsule was determined to be 0.93 (Table D-1). Although this normalization is strictly correct only at the capsule location, it was considered applicable to all locations in the host reactor, CR-3, and in the donor reactor, Oconee 2, because of the similarity between the reactors and calculational models (B&W 177-FA reactors have essentially the same configurations and materials.) In the calculational model, the pressure vessel and the capsule are separated by only 15 cm of water, and it is very unlikely that any significant change in accuracy would occur over that distance.

2. Vessel Fluence Extrapolation

For current operation, fluence values in the pressure vessel are calculated as described above. Extrapolation to future operation is required to predict vessel life based on minimum upper shelf energy and for calculation of pressure-temperature operation curves. Three time periods are considered: (1) to-date operation for which vessel fluence has been calculated, (2) designed future fuel cycles for which PDQ criticality calculations have been performed for fuel management analysis of reload cores, and (3) future fuel cycles for which no analyses exist. Data from time period 1 are extrapolated through time period 2 based on the premise that ex-core flux is proportional to the fast flux that escapes the core boundary. Thus, for the vessel,

$$\phi_{v,x} = \frac{\phi_{e,x}}{\phi_{e,R}} \times \phi_{v,R}$$

where the subscripts are defined as v = vessel, e = core escape, R = reference cycle, and x = a future fuel cycle. Core escape flux is available from PDQ output. Extrapolation from time periods 2 through 3 is based on the last fuel cycle in 2 having the same relative power distribution as an "equilibrium" cycle. Generally, the designed fuel cycles include several cycles into the future. Therefore, the last cycle in time period 2 should be representative of an "equilibrium" cycle. Data for Oconee 2 are listed in Table D-2.

This procedure is considered preferable to the alternative of assuming that lifetime fluence is based on a single, hypothetical "equilibrium" fuel cycle because it accounts for all known power distributions. In addition, it reduces errors that may result from the selection of a hypothetical "equilibrium" cycle.

Table D-1. Capsule Normalization Constant

Reaction	Measured activity, $\mu\text{Ci/g}$ ^(a)				
	A ₁ Cycle 1, OC-2	Cycles 1B and 2, CR-3	A CR-3 irradiation only	B calculated activity, $\mu\text{Ci/g}$	C = A/B normalization constant ^(c)
$^{54}\text{Fe}(n,p)^{54}\text{Mn}$	1.82(+1)	9.52(+2)	9.34(+2)	1.16(+3)	0.80
$^{58}\text{Ni}(n,p)^{58}\text{Co}$	7 (-4)	1.94(+3)	1.94(+3)	2.49(+3)	0.78
$^{238}\text{U}(n,f)^{137}\text{Cs}$	1.1	4.45	3.35	3.24	1.03
$^{277}\text{Np}(n,f)^{137}\text{Cs}$	6.1	2.42(+1)	1.81(+1)	2.09(+1)	0.87
$^{238}\text{U}(n,f)^{103}\text{Ru}$	1 (-9)	1.17(+2)	1.17(+2)	1.41(+2)	0.84
$^{238}\text{U}(n,f)^{106}\text{Ru}$	9 (-1)	2.69(+1)	2.6 (+1)	2.87(+1)	0.91
$^{237}\text{Np}(n,f)^{106}\text{Ru}$	6.2	1.27(+2)	1.21(+2)	1.27(+2)	0.96
$^{238}\text{U}(n,f)^{144}\text{Ce}$	6 (-1)	5.8 (+1)	5.74(+1)	5.67(+1)	1.01
$^{237}\text{Np}(n,f)^{144}\text{Ce}$	2.6	2.81(+2)	2.78(+2)	3.09(+2)	0.90
$^{238}\text{U}(n,f)^{95}\text{Zr}$	7 (-6)	1.04(+2)	1.04(+2)	1.08(+2)	0.96
$^{237}\text{U}(n,f)^{95}\text{Zr}$	4 (-5)	6.05(+2)	6.05(+2)	7.13(+2)	0.85

(a) Average of four dosimeter wires from Table E-2.

(b) Obtained from $A = A_2 - A_1 e^{-\lambda t}$ where λ is the decay constant for the product isotope and t is calendar time from EOC-1 in Oconee 2 to EOC-2 in Crystal River 3 (1420 days).

(c) Value for irradiation in Crystal River 3 only. Average of all fission reactions (0.93) was selected as the normalization constant.

Table D-2. Extrapolation of Pressure Vessel Fluence

Cycle	Core escape flux, n/cm ² -s	Time, EFPY	Cumul. time, EFPY	Vessel flux, n/cm ² -s	Vessel fluence, n/cm ²	
					Time interval	Cumulative
1	0.482 (+14)	1.20	1.20	1.39 (+10)	5.28 (+17)	5.28 (+17)
2	0.560 (+14) ^(a)	0.76	3.73	1.57 (+10)	1.25 (+18)	1.77 (+18)
3	0.612 (+14) ^(b)	0.79				
4	0.587 (+14)	0.97				
5	0.428	1.07	4.79	1.14 (+10)	3.84 (+17)	2.16 (+18)
6	0.416	1.10	4.89	1.11 (+10)	3.84 (+17)	2.54 (+18)
7	0.425	1.15	7.04	1.13 (+10)	4.13 (+17)	2.96 (+18)
8	0.427	1.15	8.19	1.14 (+10) ^(c)	4.14 (+17)	3.37 (+18)
>8	0.427	6.80	15	1.14 (+10) ^(d)	2.46 (+18)	5.83 (+18)
>15	0.427	17	32	1.14 (+10) ^(d)	6.15 (+18)	1.20 (+19)

(a) Weighted.

(b) Avg = 0.587(+14).

(c) Value from $\frac{0.427 \times 10^{14}}{0.587 \times 10^{14}} \times (1.57 \times 10^{10}) = 1.14 \times 10^{10}$.

(d) Cycle 8 assumed to be equilibrium cycle for future operation.

APPENDIX E
Capsule Dosimetry Data

Table E-1 lists the composition of the threshold detectors and the cadmium thicknesses used to reduce competing thermal reactions. Table E-2 shows the capsule OCII-A measured activity per gram of target material (i.e., per gram of uranium, nickel, etc.) corrected for the wait time between irradiation and counting. Activation cross sections for the various materials were flux-weighted with a ^{235}U fission spectrum (Table E-3).

Table E-1. Detector Composition and Shielding

<u>Monitors</u>	<u>Shielding</u>	<u>Reaction</u>
10.38% U-Al	Cd-Ag 0.02676" Cd	$^{238}\text{U}(n,f)$
1.44% Np-Al	Cd-Ag 0.02676" Cd	$^{237}\text{Np}(n,f)$
Ni 100%	Cd-Ag 0.02676" Cd	$^{58}\text{Ni}(n,p)^{58}\text{Co}$
0.56% Co-Al	Cd-0.040" Cd	$^{59}\text{Co}(n,\gamma)^{60}\text{Co}$
0.56% Co-Al	None	$^{59}\text{Co}(n,\gamma)^{60}\text{Co}$
Fe 100%	None	$^{54}\text{Fe}(n,p)^{54}\text{Mn}$

Table E-2. Capsule OCII-A Dosimeter Activity Measurements

Dosimeter material	Post-irr weight, g	Reaction	Radio-nuclide	Nuclide activity, μCi	Specific activity, $\mu\text{Ci/g}$	Activity, $\mu\text{Ci/g}$ of target
<u>Dosimeter AD-1</u>						
Co-Al (bare)	0.0154	$^{59}\text{Co}(n,\gamma)$	^{60}Co	20.31	1320	236,000
Co-Al (Cd)	0.0128	$^{59}\text{Co}(n,\gamma)$	^{60}Co	14.08	1100	196,000
Ni	0.1309	$^{58}\text{Ni}(n,p)$	^{58}Co	151.1	1150	1,700
		$^{60}\text{Ni}(n,p)$	^{60}Co	0.3732	2.85	10.9
	0.1513	$^{54}\text{Fe}(n,p)$	^{54}Mn	7.526	49.7	855
		$^{56}\text{Fe}(n,\gamma)$	^{59}Fe	22.94	152	45,900
^{238}U -Al	0.0329	$^{238}\text{U}(n,F)$	^{95}Zr	0.3094	9.40	91.3
			^{103}Ru	0.3003	9.13	88.6
			^{106}Ru	0.0841	2.56	24.8
			^{137}Cs	0.01506	0.458	4.44
			^{144}Ce	0.1773	5.39	52.3
^{237}Np -Al	0.0291	$^{237}\text{Np}(n,F)$	^{95}Zr	0.2321	7.98	554
			^{103}Ru	--	--	--
			^{106}Ru	0.0408	1.40	97.4
			^{137}Cs	0.009562	0.329	22.8
			^{144}Ce	0.1061	3.65	253
<u>Dosimeter AD-2</u>						
Co-Al (bare)	0.0145	$^{59}\text{Co}(n,\gamma)$	^{60}Co	21.07	1453	259,000
Co-Al (Cd)	0.0145	$^{59}\text{Co}(n,\gamma)$	^{60}Co	17.13	1180	211,000
Ni	0.1330	$^{58}\text{Ni}(n,p)$	^{58}Co	177.0	1331	1,960
		$^{60}\text{Ni}(n,p)$	^{60}Co	0.3748	2.82	10.8
Fe	0.1543	$^{54}\text{Fe}(n,p)$	^{54}Mn	8.754	56.7	975
		$^{56}\text{Fe}(n,\gamma)$	^{59}Fe	28.11	182	55,200
^{238}U -Al	0.0433	$^{238}\text{U}(n,F)$	^{95}Zr	0.5158	11.9	116
			^{103}Ru	0.6173	14.3	138
			^{106}Ru	0.118	2.72	26.5
			^{137}Cs	0.01957	0.452	4.39
			^{144}Ce	0.2738	6.32	61.4
^{237}Np -Al	0.0239	$^{237}\text{Np}(n,F)$	^{95}Zr	0.2054	8.59	597
			^{103}Ru	--	--	--
			^{106}Ru	0.0534	2.23	155
			^{137}Cs	0.007954	0.333	23.1
			^{144}Ce	0.09692	4.06	282

Table E-2. (Cont'd)

Dosimeter material	Post-irr weight, g	Reaction	Radio-nuclide	Nuclide activity, μCi	Specific activity, $\mu\text{Ci/g}$	Activity, $\mu\text{Ci/g}$ of target
<u>Dosimeter AD-3</u>						
Co-Al (bare)	0.0153	$^{59}\text{Co}(n,\gamma)$	^{60}Co	20.49	1340	239,000
Co-Al (Cd)	0.0133	$^{59}\text{Co}(n,\gamma)$	^{60}Co	14.86	1120	200,000
Ni	0.1341	$^{58}\text{Ni}(n,p)$	^{58}Co	150.9	1120	1,660
		$^{60}\text{Ni}(n,p)$	^{60}Co	0.3661	2.73	10.4
Fe	0.1505	$^{54}\text{Fe}(n,p)$	^{54}Mn	7.146	47.5	816
		$^{58}\text{Fe}(n,\gamma)$	^{59}Fe	24.55	163	49,400
^{238}U -Al	0.0364	$^{238}\text{U}(n,f)$	^{95}Zr	0.3420	9.40	91.2
			^{103}Ru	0.4051	11.1	108
			^{106}Ru	0.0850	2.34	22.7
			^{137}Cs	0.01483	0.407	3.96
			^{144}Ce	0.1844	5.07	49.2
^{237}Np -Al	0.0485	$^{237}\text{Np}(n,f)$	^{95}Zr	0.3481	7.18	498
			^{103}Ru	--	--	--
			^{106}Ru	0.0706	1.46	101
			^{137}Cs	0.01503	0.310	21.5
			^{144}Ce	0.1645	3.39	236
<u>Dosimeter AD-4</u>						
Co-Al (bare)	0.0162	$^{59}\text{Co}(n,\gamma)$	^{60}Co	29.27	1810	323,000
Co-Al (Cd)	0.0133	$^{59}\text{Co}(n,\gamma)$	^{60}Co	20.50	1540	275,000
Ni	0.1342	$^{58}\text{Ni}(n,p)$	^{58}Co	222.3	1660	2,440
		$^{60}\text{Ni}(n,p)$	^{60}Co	0.4599	3.4	13.1
Fe	0.1520	$^{54}\text{Fe}(n,p)$	^{54}Mn	10.27	67.6	1,160
		$^{58}\text{Fe}(n,\gamma)$	^{59}Fe	34.66	228	69,100
^{238}U -Al	0.0349	$^{238}\text{U}(n,f)$	^{95}Zr	0.4271	12.2	119
			^{103}Ru	0.4849	13.9	135
			^{106}Ru	0.121	3.47	33.7
			^{137}Cs	0.01803	0.517	5.02
			^{144}Ce	0.2485	7.12	69.1
^{237}Np -Al	0.0486	$^{237}\text{Np}(n,f)$	^{95}Zr	0.5393	11.1	771
			^{103}Ru	--	--	--
			^{106}Ru	0.109	2.24	156
			^{137}Cs	0.02065	0.425	29.5
			^{144}Ce	0.2475	5.09	354

Table E-3. Dosimeter Activation Cross Sections^(a)

G	Energy range, Mev	Cross sections, b/atom			
		²³⁷ Np	²³⁸ U	⁵⁸ Ni	⁵⁴ Fe
1	12.2 - 15	2.323	1.050	4.830(-1)	4.133(-1)
2	10.0 - 12.2	2.341	9.851(-1)	5.735(-1)	4.728(-1)
3	8.18 - 10.0	2.309	9.935(-1)	5.981(-1)	4.772(-1)
4	6.36 - 8.18	2.093	9.110(-1)	5.921(-1)	4.714(-1)
5	4.96 - 6.36	1.541	5.777(-1)	5.223(-1)	4.321(-1)
6	4.06 - 4.96	1.532	5.454(-1)	4.146(-1)	3.275(-1)
7	3.01 - 4.06	1.614	5.340(-1)	2.701(-1)	2.193(-1)
8	2.46 - 3.01	1.689	5.272(-1)	1.445(-1)	1.080(-1)
9	2.35 - 2.46	1.695	5.298(-1)	9.154(-2)	5.613(-2)
10	1.83 - 2.35	1.677	5.313(-1)	4.856(-2)	2.940(-2)
11	1.11 - 1.83	1.596	2.608(-1)	1.180(-2)	2.948(-3)
12	0.55 - 1.11	1.241	9.845(-3)	6.770(-4)	6.999(-5)
13	0.111 - 0.55	2.34(-1)	2.432(-4)	1.174(-6)	1.578(-8)
14	0.0033 - 0.111	6.928(-3)	3.616(-5)	1.023(-7)	1.389(-9)

(a) ENDF/B5 values that have been flux-weighted (over CASK energy groups) based on a ²³⁵U fission spectrum in the fast energy range plus a 1/E shape in the intermediate energy range.

APPENDIX F
References

- ¹ H. S. Palme, G. S. Carter, and C. L. Whitmarsh, Reactor Vessel Material Surveillance Program - Compliance with 10 CFR 50, Appendix H, for Oconee-Class Reactors, BAW-10100A, Babcock & Wilcox, Lynchburg, Virginia, February 1975.
- ² A. L. Lowe, Jr., et al., Analysis of Capsule from Duke Power Company Oconee Nuclear Station, Unit 2, Reactor Vessel Material Surveillance Program, BAW-1437, Babcock & Wilcox, Lynchburg, Virginia, May 1977.
- ³ G. J. Snyder and G. S. Carter, Reactor Vessel Material Surveillance Program, BAW-10006A, Rev. 3, Babcock & Wilcox, Lynchburg, Virginia, January 1975.
- ⁴ H. S. Palme and H. W. Behnke, Methods of Compliance With Fracture Toughness and Operational Requirements of Appendix G to 10 CFR 50, BAW-10046P, Babcock & Wilcox, Lynchburg, Virginia, October 1975.
- ⁵ H. S. Palme, G. S. Carter, and C. L. Whitmarsh, Reactor Vessel Material Surveillance Program - Compliance With 10 CFR 50, Appendix H, for Oconee-Class Reactors, BAW-10100A, Babcock & Wilcox, Lynchburg, Virginia, February 1975.
- ⁶ DOT3.5 - Two-Dimensional Discrete Ordinates Radiation Transport Code (CCC-276), WANL-TME-1982, Oak Ridge National Laboratory, December 1969.
- ⁷ CASK - 40-Group Coupled Neutron and Gamma-Ray Cross Section Data, DLC-23E, Radiation Shielding Information Center.
- ⁸ C. L. Whitmarsh, Pressure Vessel Fluence Analysis, BAW-1485, Babcock & Wilcox, Lynchburg, Virginia, June 1978.